AD-A044 793 COLD REGIONS RESEARCH AND ENGINEERING LAB HANOVER N H F/G 13/2
AIRBORNE SPECTRORADIOMETER DATA COMPARED WITH GROUND WATER-TURB--ETC(U)
SEP 77 C J MERRY

UNCLASSIFIED CRREL-SR-77-28 NL

1 OF 1
ADA044793

END
DATE FILMED
10-77
DDC

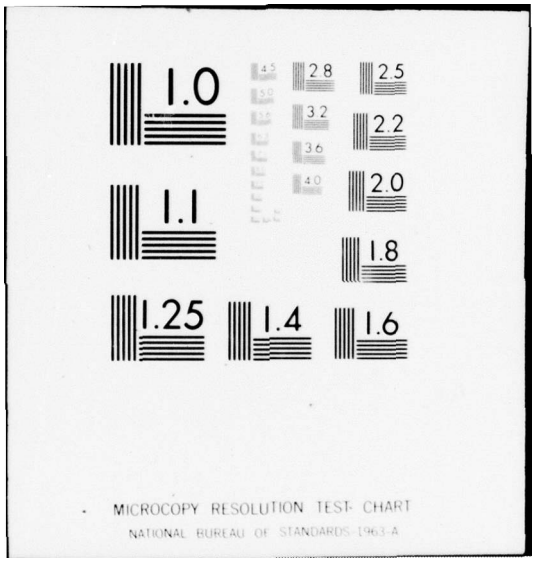
1.0
1.1
1.25
1.4
1.6
1.8
2.0
2.2
2.5
2.8
3.2
3.6
4.0
4.5
5.0
MICROCOPY RESOLUTION TEST CHART
NATIONAL BUREAU OF STANDARDS-1963-A

SR 77-28

CRREL

12 NW

Special Report 77-28

AIRBORNE SPECTRORADIOMETER DATA COMPARED WITH GROUND WATER-TURBIDITY MEASUREMENTS AT LAKE POWELL, UTAH

Correlation and Quantification of Data

Carolyn J. Merry

September 1977

CORPS OF ENGINEERS, U.S. ARMY
COLD REGIONS RESEARCH AND ENGINEERING LABORATORY
HANOVER, NEW HAMPSHIRE

Unclassified

SECURITY CLASSIFICATION OF THIS PAGE (When Data Entered)

REPORT DOCUMENTATION PAGE		READ INSTRUCTIONS BEFORE COMPLETING FORM
1. REPORT NUMBER Special Report 77-28	2. GOVT ACCESSION NO.	3. RECIPIENT'S CATALOG NUMBER
4. TITLE (and Subtitle) AIRBORNE SPECTRORADIOMETER DATA COMPARED WITH GROUND WATER-TURBIDITY MEASUREMENTS AT LAKE POWELL, UTAH. Correlation and Quantification of Data		5. TYPE OF REPORT & PERIOD COVERED 6. PERFORMING ORG. REPORT NUMBER
7. AUTHOR(s) Carolyn J. Merry		8. CONTRACT OR GRANT NUMBER(s) NASA Grant NSG-5014
9. PERFORMING ORGANIZATION NAME AND ADDRESS U.S. Army Cold Regions Research and Engineering Laboratory Hanover, New Hampshire 03755		10. PROGRAM ELEMENT, PROJECT, TASK AREA & WORK UNIT NUMBERS
11. CONTROLLING OFFICE NAME AND ADDRESS National Aeronautics and Space Administration Goddard Institute for Space Studies 2880 Broadway, New York, New York 10025		12. REPORT DATE September 1977 13. NUMBER OF PAGES 43
14. MONITORING AGENCY NAME & ADDRESS (if different from Controlling Office)		15. SECURITY CLASS. (of this report) Unclassified 15a. DECLASSIFICATION/DOWNGRADING SCHEDULE

16. DISTRIBUTION STATEMENT (of this Report)

Approved for public release; distribution unlimited.

17. DISTRIBUTION STATEMENT (of the abstract entered in Block 20, if different from Report)

18. SUPPLEMENTARY NOTES

This study was made possible by a NASA Grant through Dartmouth College to CRREL.

19. KEY WORDS (Continue on reverse side if necessary and identify by block number)

Airborne spectroradiometer data
Groundwater-turbidity measurements
Lake Powell, Utah
Multispectral data
Remote sensing
Water quality measurements

20. ABSTRACT (Continue on reverse side if necessary and identify by block number)

During the past three years there has been a renewed interest in the methodology and procedures used to monitor water quality in fresh and salt water regimes. However, there still exists a need to calculate quantitatively the amount of surface turbidity by remote sensing methods to provide rapid and synoptic water quality surveys. Recently a 500-channel airborne spectroradiometer, which may provide a quantitative means of comparing high resolution multispectral data to water quality parameters, has been designed at the NASA Goddard Institute for Space

DD FORM 1 JAN 73 1473 EDITION OF 1 NOV 65 IS OBSOLETE

Unclassified

SECURITY CLASSIFICATION OF THIS PAGE (When Data Entered)

Studies (GISS). The objective of this study is to correlate and quantify the airborne spectroradiometer multispectral data to ground truth water quality measurements obtained in Lake Powell, Utah, during June 1975.

A ground truth water sampling program was accomplished during 9-16 June 1975 for correlation to an aircraft spectroradiometer flight. Field measurements were taken of percentage of transmittance, surface temperature, pH and secchi disk depth. Also, percentage of transmittance was measured in the laboratory for the water samples. In addition, electron micrographs and suspended sediment concentration data were obtained of selected water samples located at Hite Bridge (Mile 171), Mile 168, Mile 150 and Bullfrog Bay (Mile 122). Airborne spectroradiometer spectra were selected which correlated to the Hite Bridge (Mile 171), Mile 168, Mile 150 and Bullfrog Bay (Mile 122) test sites.

Analysis of the data leads to the following conclusions: (a) as the secchi disk depth measurement of light extinction decreased, the reflected radiance measured by the airborne spectroradiometer increased; (b) as the percentage of transmittance of the water samples decreased, the reflected radiance increased; (c) as the insoluble particulate concentration (mg/1) increased, the reflected radiance increased, at least in the 1-80 mg/1 range; (d) the reflected radiance in the near infrared region (0.76-0.91μ) always increased as the insoluble particulate matter concentration (mg/1) increased; and (e) when a spectral peak occurred at a wavelength of 0.58μ, the peak reflected radiance varied with the insoluble particulate matter concentration as follows:

Peak reflected radiance (mW/cm^2 sr)	Concentration (mg/1)
0.0001 - 0.0027	1 - 5
0.0027 - 0.0047	5 - 44
0.0047 - 0.0060	44 - 77

An interpretation of the Hite Bridge (Mile 171), Mile 168 and Mile 150 aircraft spectra indicated a similar mineralogic source due to the occurrence of a 0.58μ spectral peak and 0.64μ shoulder. The decrease of reflected radiance throughout the visible and near infrared regions for the three sites corresponds to a quantitative decrease of suspended sediment concentration from 77.2 mg/1 to 41.1 mg/1 to 5.9 mg/1, respectively.

Analysis of the aircraft spectra shows that quantification of turbidity in water bodies is feasible. The technique is especially effective when the turbidity in the water is derived from the same source as was the case in the Hite Bridge (Mile 171), Mile 168 and Mile 150 sites, which are all located along the main Colorado River channel. The quantification consists in plotting the measured spectral reflected radiance, at the key wavelengths of 0.58μ, 0.64μ and 0.79μ, with the measured concentration of particles in the water. The resulting graphs can be used as a quantitative measure of particle content throughout this reach of the Colorado River channel, as long as the spectral peak at 0.58μ and shoulder at 0.64μ are present, indicating a similar mineralogic source.

The relationship should be tested for uniqueness and reproducibility to complete the study of the quantitative usefulness of reflected radiances in monitoring water quality. A combination of theoretical work and laboratory or controlled field experiments would provide a solid foundation for further development of remote sensing as a practical tool in the monitoring of water quality.

PREFACE

This report was prepared by Carolyn J. Merry, Geologist, of the Earth Sciences Branch, Research Division, U.S. Army Cold Regions Research and Engineering Laboratory (CRREL). The study was made possible through a NASA Grant (#NSG-5014) to Dartmouth College and by a CRREL Work Unit entitled, "CRREL-NASA-Dartmouth Cooperative Study at Lake Powell." The facilities of the US Army Cold Regions Research and Engineering Laboratory, NASA Goddard Institute for Space Studies (GISS), and Dartmouth College were used throughout the course of the study.

The author extends her appreciation to Dr. Harlan L. McKim (CRREL) for his support, guidance and technical review of the study; to Dr. Robert Jastrow (NASA GISS) for his guidance, particularly in the theoretical modeling aspects, and technical review; to Dr. Stephen G. Ungar (NASA GISS) for technical review and development of the computer algorithms for the airborne spectroradiometer data through support of the GISS programming staff; to Dr. Charles Drake (Dartmouth College) and Dr. Robert C. Reynolds (Dartmouth College) for technical review and field assistance during the ground truth program; to Ronald T. Atkins (CRREL) for technical review; and to Daniel C. Leggett (CRREL) for assistance in the determination of suspended sediment concentration.

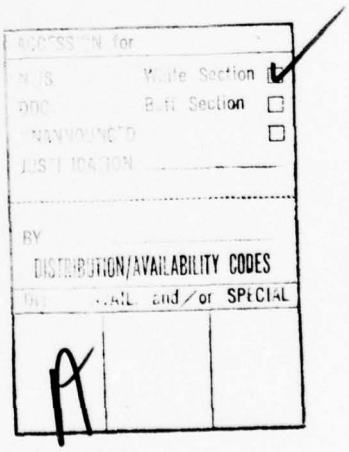

CONTENTS

ILLUSTRATIONS

TABLES

INTRODUCTION

During the past three years there has been a renewed interest in the methodology and procedures used to monitor water quality in fresh and salt water regimes. However, there still exists a need to calculate quantitatively the amount of surface turbidity by remote sensing methods to provide rapid and synoptic water quality surveys.

Many studies have been accomplished that concern only the extraction of qualitative information on turbidity derived from analysis of multispectral data. However, recently a 500-channel airborne spectroradiometer which may provide a quantitative means of comparing high resolution multispectral data to water quality parameters has been designed at the NASA Goddard Institute for Space Studies (GISS). Also, theoretical models are being examined that will predict spectral response curves based on varying the size, optical properties and density of particulate matter in the water and atmospheric conditions (Hansen, 1976). A more extensive treatment of the theoretical optical properties of water and previous multispectral analysis for water quality can be found in Appendix A. The primary objective of this study was to correlate and quantify airborne spectroradiometer multispectral data with ground truth water-turbidity measurements obtained at Lake Powell, Utah, during June 1975.

AIRBORNE SPECTRORADIOMETER INSTRUMENT

The 500-channel airborne spectroradiometer measures ground reflectance in terms of radiance, mW/cm^2 sr*, from about 0.42-1.0μ and has a spectral resolution of approximately 14Å. The aircraft instrument system comprises a Princeton Applied Research Optical Multichannel Analyzer (OMA), which drives a silicon vidicon detector coupled to a Jarrel-Ash 0.33-m spectrometer, and a computer compatible tape recorder (Collins 1976).

Collecting optics image a ground target on an entrance slit of the spectrometer. The radiation is collimated through the entrance slit, dispersed by a grating and refocused on the silicon vidicon detector. The vidicon detector samples the spectral data in 500-wavelength intervals at the rate of 64μ seconds per channel and 32 milliseconds per frame. Each scan line is amplified, digitized and stored on tape. The parallel digital data output is transmitted to a computer formatted eight track magnetic tape recorder for subsequent computer processing of the multispectral data. An interface monitors these data for errors and triggers a ground truth photographic camera on every tenth spectrum. The aircraft measurements are calibrated against a standard tungsten lamp. Also, frequency calibration is accomplished by use of a krypton lamp to determine the instrument spectral channel width and wavelength scale. Further details on the spectroradiometer instrument can be obtained from the reference by Collins (1976).

---

*Milliwatts per square centimeter per steradian.

APPROACH

June 1975 field trip to Lake Powell, Utah

A field trip was conducted to Lake Powell during 9-16 June 1975. The primary objective was to obtain field measurements of turbidity during an aircraft overflight of the spectroradiometer. Water samples were taken from the Rincon region north to the Dark Canyon area of Lake Powell (Fig. 1). Field temperatures and pH values were also recorded (Reynolds, 1976).

Photographs of the water surface were taken. In addition, wind speed data and characteristics of atmospheric conditions such as cloud cover and air temperature were noted. Secchi disk depth measurements were taken during the field trip.

Field and laboratory measurements of turbidity

Percentage of light transmittance. Values of percentage of light transmittance, a measure of water turbidity, were obtained in the field using a Bausch and Lomb Minispec 20 instrument. These values were checked in the laboratory using a Coleman Model 14 Universal Spectrophotometer. The Coleman 14 spectrophotometer allows selection of a single wavelength for transmittance measurements. For this study 13 wavelengths between 0.400 and 0.825μ were used. Photometric measurement is made first with a reference sample and then with an unknown sample placed in the light beam. The ratio of the two intensity values is a measure of the relative transmittance of the sample at a specific wavelength. In this study a cuvette (1 cm diameter) of distilled water was used as the reference sample.

The method of the light transmittance measurement from the spectrophotometer is illustrated in Figure 2. The difference in concentration between the reference and the sample is determined by measuring the relative intensities of the exit beam (B), first with the reference and then with the sample in position (Coleman Instruments, 1969). In this study the intensity of the exit beam decreased from the original value of "B_r" to a lower value "B_s" because of the constituents in the unknown sample. The transmittance value is a measure of the difference in concentration, not the absolute concentration, between the reference sample of distilled water and the unknown sample. As a result, the transmittance measurement is dependent only on the nature and amount of the extra constitutents in the water.

Secchi disk depth data. The procedure for obtaining the Secchi disk depth measurements was to observe the depth at which a white circular disk inserted downward from the water surface just disappeared from view (Hutchinson, 1957). The secchi disk depth is only a qualitative measurement of turbidity yielding approximate information about water clarity.

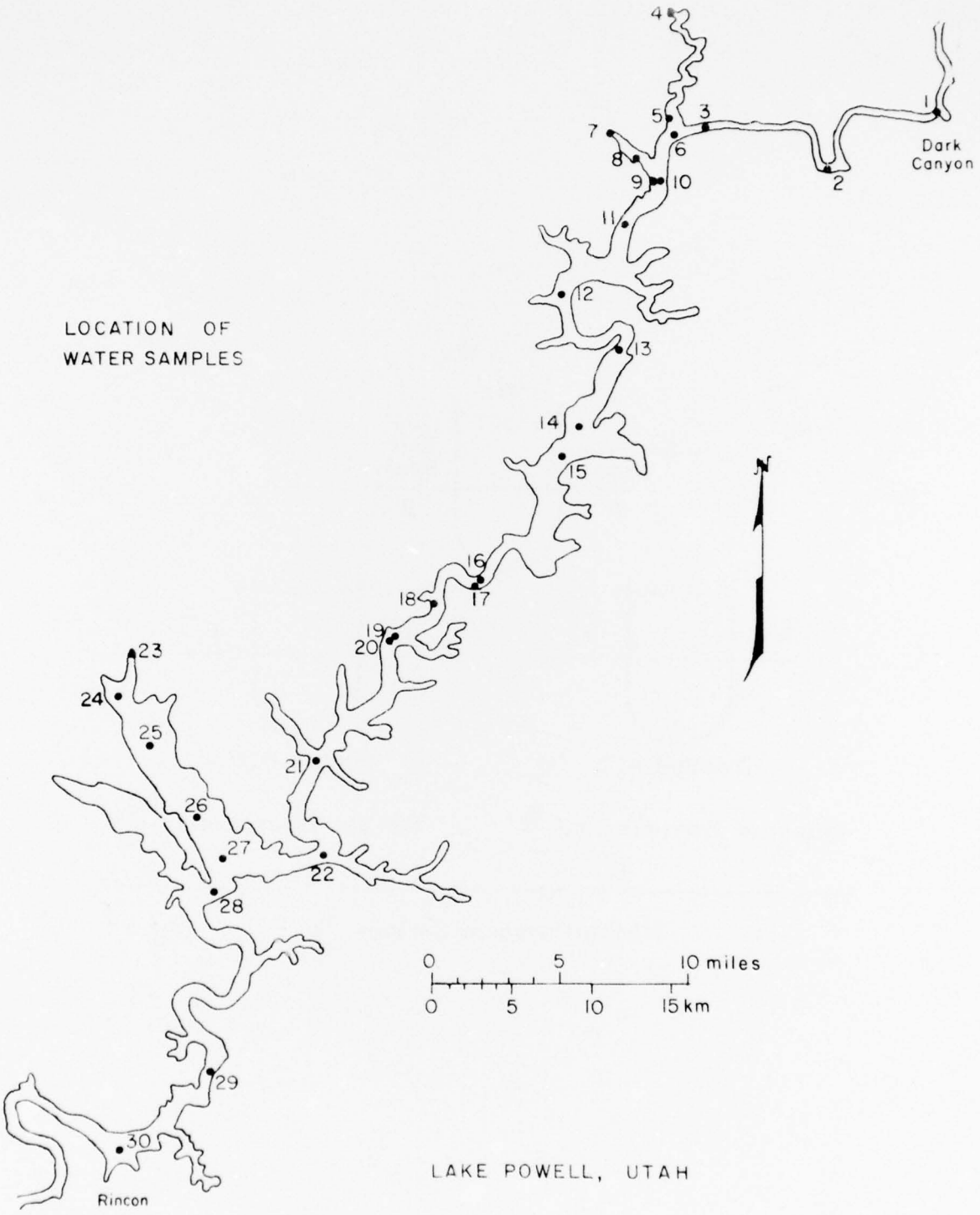

Figure 1. Location map of Lake Powell water samples (June 1975).

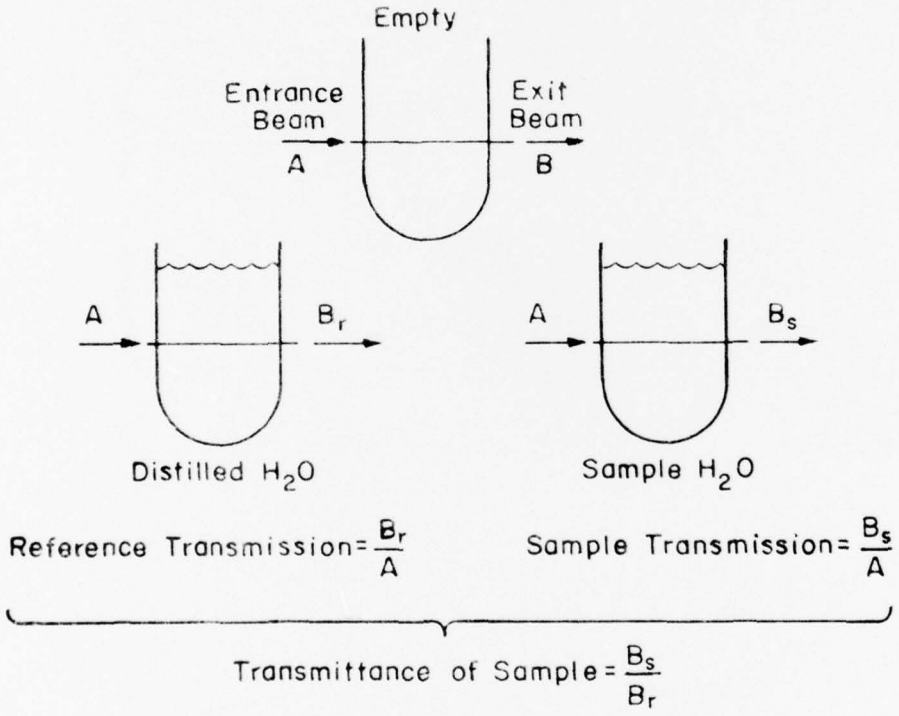

Figure 2. Light transmittance measurement using spectrophotometer technique.

Electron microscopy. A 5 mg sample of Bullfrog Bay (Mile 122) water and 1 mg samples from Mile 150, Mile 168 and Hite Bridge (Mile 171) water (see Fig. 3) were placed on an electron microscope grid covered with collodion film and dried in air. Each sample measured 2 mm in diameter and was approximately 10 μm thick. Polystyrene latex particles of 1.305μ diameter were added for scale reference. The sample was then placed in a vacuum chamber and shadowed with a chromium vapor. Electron micrographs were obtained for these samples at a 3675x magnification (Kumai, 1976).

Concentration, filtered. A 50 ml aliquot of the Bullfrog Bay (Mile 122), Mile 150, Mile 168 and Hite Bridge (Mile 171) water samples (see Fig. 3) was passed through a 0.45μ Millipore filter. Each filtrate was washed several times to ensure removal of soluble salts. The filter papers were oven dried and the remaining particulate matter was weighed.

Airborne spectroradiometer measurements

Airborne spectroradiometer flights were accomplished over Lake Powell on 16 and 23 June 1975 (Fig. 4). Table I shows the time of the multispectral data acquisition. The instrument used in these flights was the 500-channel spectroradiometer designed at the NASA Goddard Institute for Space Studies, New York, New York (Collins, 1976). The aircraft flights were flown in conjunction with the ground truth water sampling program. The aircraft was flown at approximately 2000 ft with the accumulation mode setting on the spectroradiometer providing for a 60x120-ft ground coverage.

Table I. Acquisition times of the airborne spectroradiometer data (June 1975).

Flight	Location	Day	Hour of Day
C'-C3	Bullfrog Bay	16 June	1005
1 s-n	Good Hope	23 June	0953
1A n-s	Good Hope	23 June	0833
4 s-n	Castle Butte	23 June	0857
4A s-n	Castle Butte	23 June	0848
5 s-n	Hite	23 June	0905
6 n-s	Dirty Devil	23 June	0914
10 w-e	Narrow Canyon	23 June	0950

Due to aircraft malfunction the majority of the spectroradiometer flights occurred approximately one week later than the ground truth sampling program (Table I and App B). However, it was anticipated that the interpretations of the airborne spectroradiometer data would be correlative to the ground truth taken one week earlier. The conditions of Lake Powell at the selected test sites would not change significantly during this period. A time scale on an order of magnitude of weeks or months is characteristic for changes in the Lake Powell water system. Also, climatological data showed that rainfall was insignificant during this two-week period (NOAA, 1975).

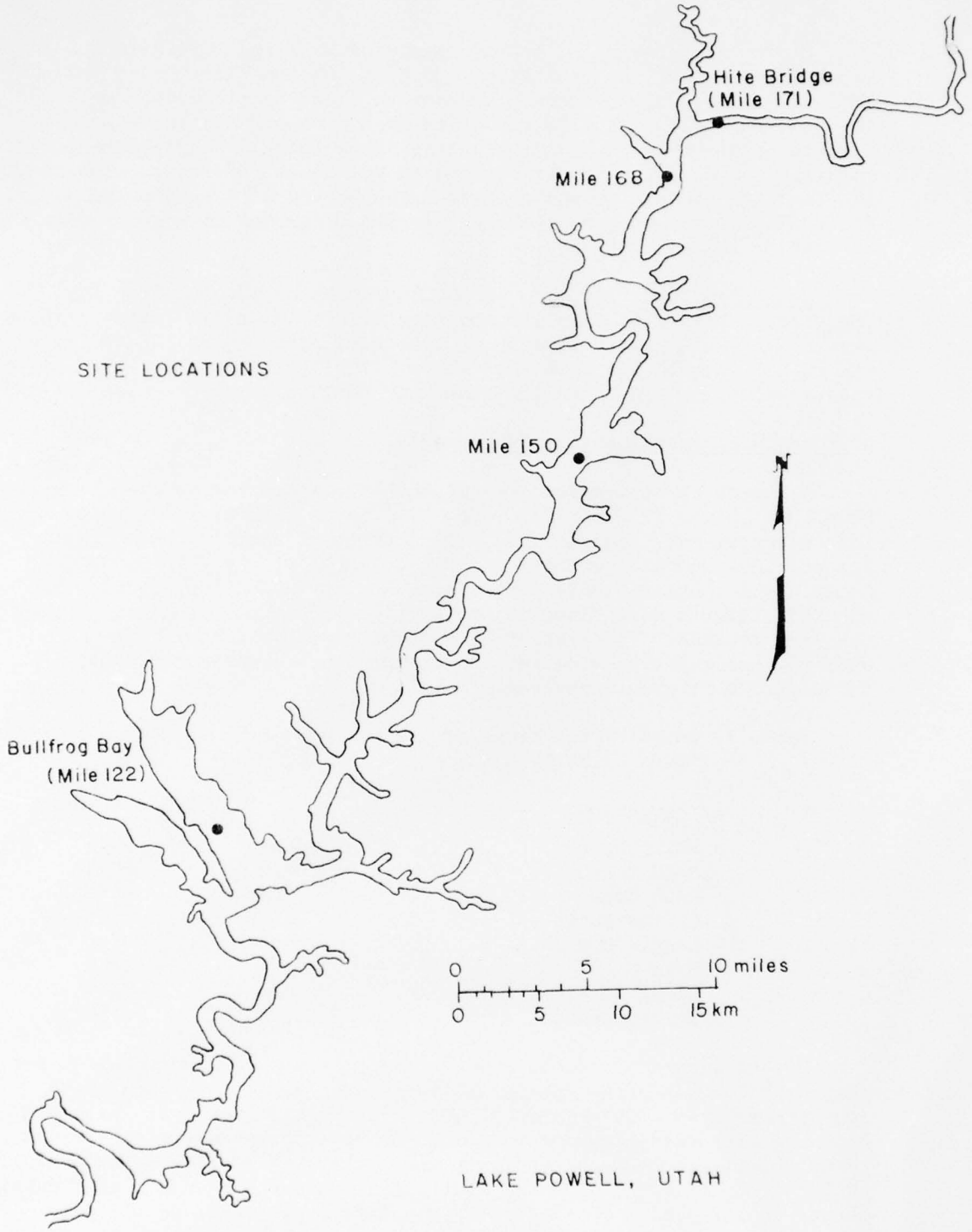

Figure 3. Site location map of selected water samples obtained at Lake Powell, Utah (June 1975).

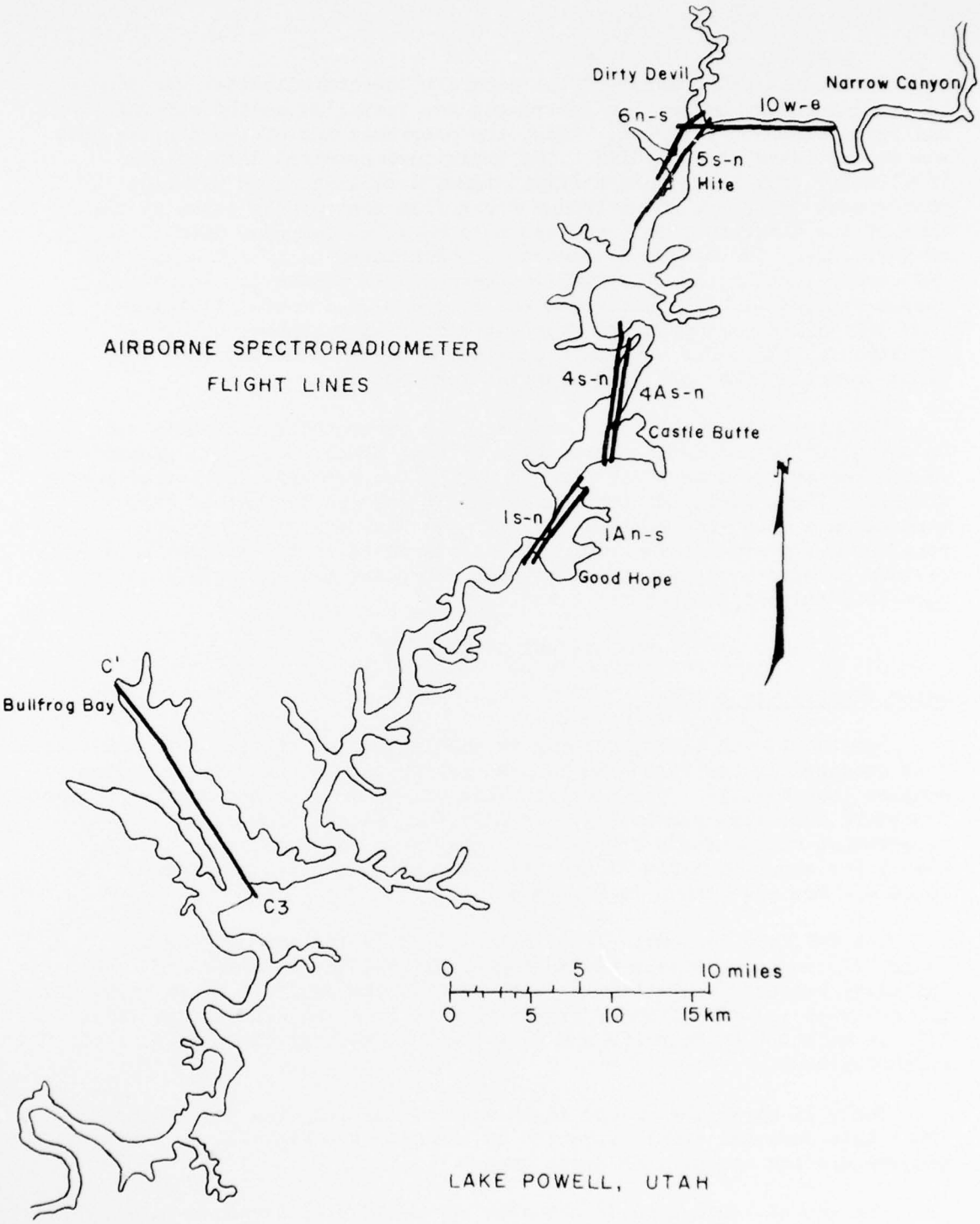

Figure 4. Location map of airborne spectroradiometer flights over Lake Powell, Utah (June 1975).

Instrument calibration of the aircraft spectroradiometer was done in the laboratory before the instrument was installed on the aircraft and again after it returned. Also, the preprocessing of the digital data was accomplished at NASA GISS. The individual spectral data points (60x120-ft) from the aircraft flight lines were located on 9x9-inch photographs using the 35 mm ground truth film photography taken at the time of the aircraft flight and the preprocessing computer data output as reference. The aircraft spectra were displayed on a Tektronix 4012 CRT terminal using the GISS CRJE (Conversational Remote Job Entry) computer program. Interactive access to the GISS computer facility (IBM 360/95) was accomplished over a direct line telephone to GISS. A Tektronix 4632 video copy unit provided a means to obtain hard copy plots from the Tektronix 4012 graphics terminal.

The aircraft spectra produced were not corrected for effects such as sun glint, atmospheric attenuation or wind speed. However, precautions were taken to minimize these effects during the aircraft spectroradiometer flights. These included obtaining aircraft spectra during the early morning on a clear day with little wind and when sun glint was not considered a problem. Therefore, the differences in the spectra between various locations in Lake Powell should represent mainly variations in turbidity and not atmospheric effects.

RESULTS AND DISCUSSION

Water transmittance data

Tables BII and BIII (App B) give tabulations of the light transmittance data obtained in the field and laboratory for all the Lake Powell water samples (see Fig. 1). These values were obtained using the spectrophotometer procedure described previously. In addition, secchi disk depth, pH and temperature measurements taken during the field reconnaissance at Lake Powell are shown in Table BI (App B). Secchi disk depth measurement locations are also shown in Figure 5.

The Bullfrog Bay (Mile 122), Mile 150, Mile 168 and Hite Bridge (Mile 171) areas were selected to represent low, intermediate and high turbidity regions, respectively (Fig. 3). In the analysis it is important to note that the direction of stream flow is from the Hite Bridge (Mile 171) to Mile 168 to Mile 150 and past the Bullfrog Bay (Mile 122) tributary area.

Table II shows the ground truth data of the selected water samples. These data included sample location on the map (see Fig. 1), pH, surface temperature and secchi disk depth data.

The ground truth data do not show appreciable differences in pH, but all values were above 8.0 indicating a highly basic water environment.

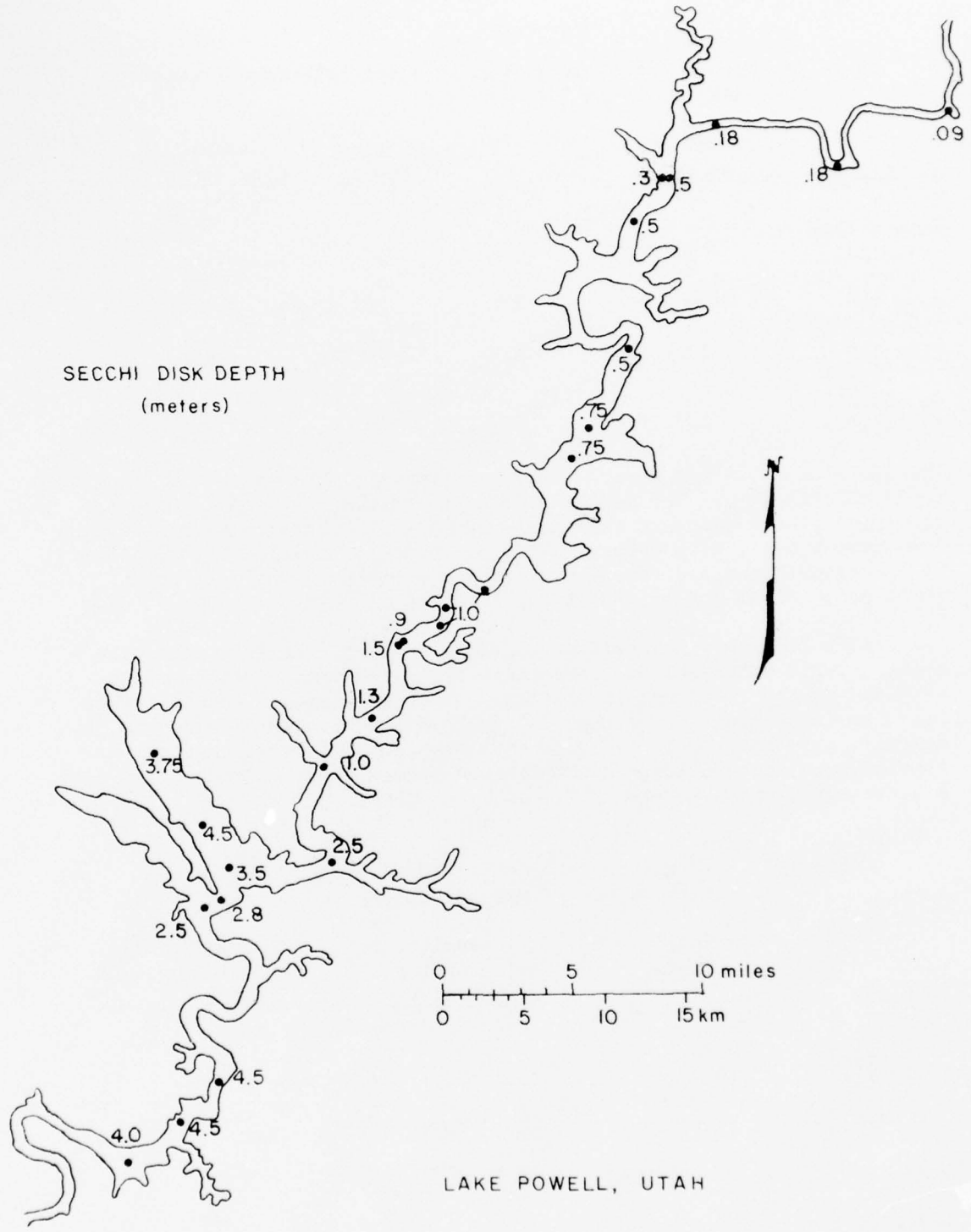

Figure 5. Secchi disk depth measurements (meters) of Lake Powell (June 1975).

Table II. Ground truth data from selected Lake Powell water samples (June 1975).

Location	Location on map	pH	Surface temp. (°C)	Secchi disk depth (m)
Hite Bridge (Mile 171)	3	8.2	18	0.18
Mile 168	9	8.5	18	0.30
Mile 150	15	8.6	20	0.75
Bullfrog Bay (Mile 122)	26	8.6	23	4.50

The temperature values were relatively warm varying from 18.0°C (64.4°F) to 23.0°F (73.4°F). The secchi disk depth data varied appreciably for the four areas. Although this measurement is only qualitative the value does give a subjective determination of water turbidity. The turbidity in the water decreased from very turbid conditions at Hite Bridge (0.18 m) to clear conditions at Bullfrog Bay (4.50 m).

Table III shows the surface turbidity data of the four test site areas. These data included percentage of transmittance measurements obtained in the field and laboratory. The percentage of transmittance measured in the laboratory showed higher values than the field data; however, the same trends occurred with both sets of measurements. At shorter wavelengths, lower transmittance values occurred because of high scattering at short wavelengths.

Table III. Surface tubidity data from selected Lake Powell water samples (June 1975).

Location	Transmittance (field) %		Transmittance (laboratory) %			Transmittance (transmissometer) %
	0.4μ	0.7μ	0.4μ	0.7μ	0.8μ	
Hite Bridge (Mile 171)	18	45	39.2	58.7	63.3	65
Mile 168	44	77	64.1	79.5	82.1	80
Mile 150	79	98	89.7	98.1	97.9	93
Bullfrog Bay (Mile 122)	90	98	95.4	99.0	99.2	99

One reason for the difference between the field and laboratory measurements can be attributed to the instrumentation as two different kinds of instruments were used. In addition, a sample with many small particles with a large total surface area would result in a lower percentage of transmittance such as measured in the field. The particulate matter in the water may have flocculated by the time the water sample was brought into the laboratory. As a result, the same water sample would show a higher percentage of transmittance because the fewer larger-sized particles with less surface area would allow more light to pass through the sample.

The percentage of transmittance data correlated well with other surface turbidity data taken on 14 June 1975 which indicated the same relationship of turbidity (Johnson and Merritt, 1975). These data were obtained by using a Hydroproducts transmissometer which was lowered into the surface water (Table III). The instrument is calibrated to an absolute value of 92% before and after each measurement using a light beam source. For example, if the instrument reads 100% in water, this indicates very clean water due to the refractive index properties between water and air.

The percentage of transmittance data taken in the field and laboratory correlate with the secchi disk depth and transmissometer measurements and show that the percentage of transmittance, secchi disk depth and transmissometer values increased from the very turbid Hite Bridge area to the relatively clear Bullfrog Bay area (Tables II, III). These ground truth data indicate differences in surface turbidity for the four test sites which should be reflected in the aircraft spectra.

Airborne spectroradiometer data

The airborne spectroradiometer data used for analysis were obtained from the following flight lines (see Fig. 4): C'-C3 (Bullfrog Bay), 1 and 1A (Good Hope), 4 and 4A (Castle Butte), 5 (Hite), 6 (Dirty Devil) and 10 (Narrow Canyon). Figure 6 shows aircraft spectra selected from these flight lines and gives representative data of the water samples obtained at the Hite Bridge (Mile 171), Mile 168, Mile 150 and Bullfrog Bay (Mile 122) locations. Table IV shows the time of day, date and sun angle elevation associated with each aircraft spectrum.

Table IV. Time of day, date and sun angle elevation associated with selected Lake Powell aircraft spectra (June 1975).

Location	Time of day	Date	Sun angle elevation (degrees)
Hite Bridge (Mile 171)	0950	23 June	42.7
Mile 168	0905	23 June	33.7
Mile 150	0833	23 June	27.4
Bullfrog Bay (Mile 122)	1005	16 June	45.6

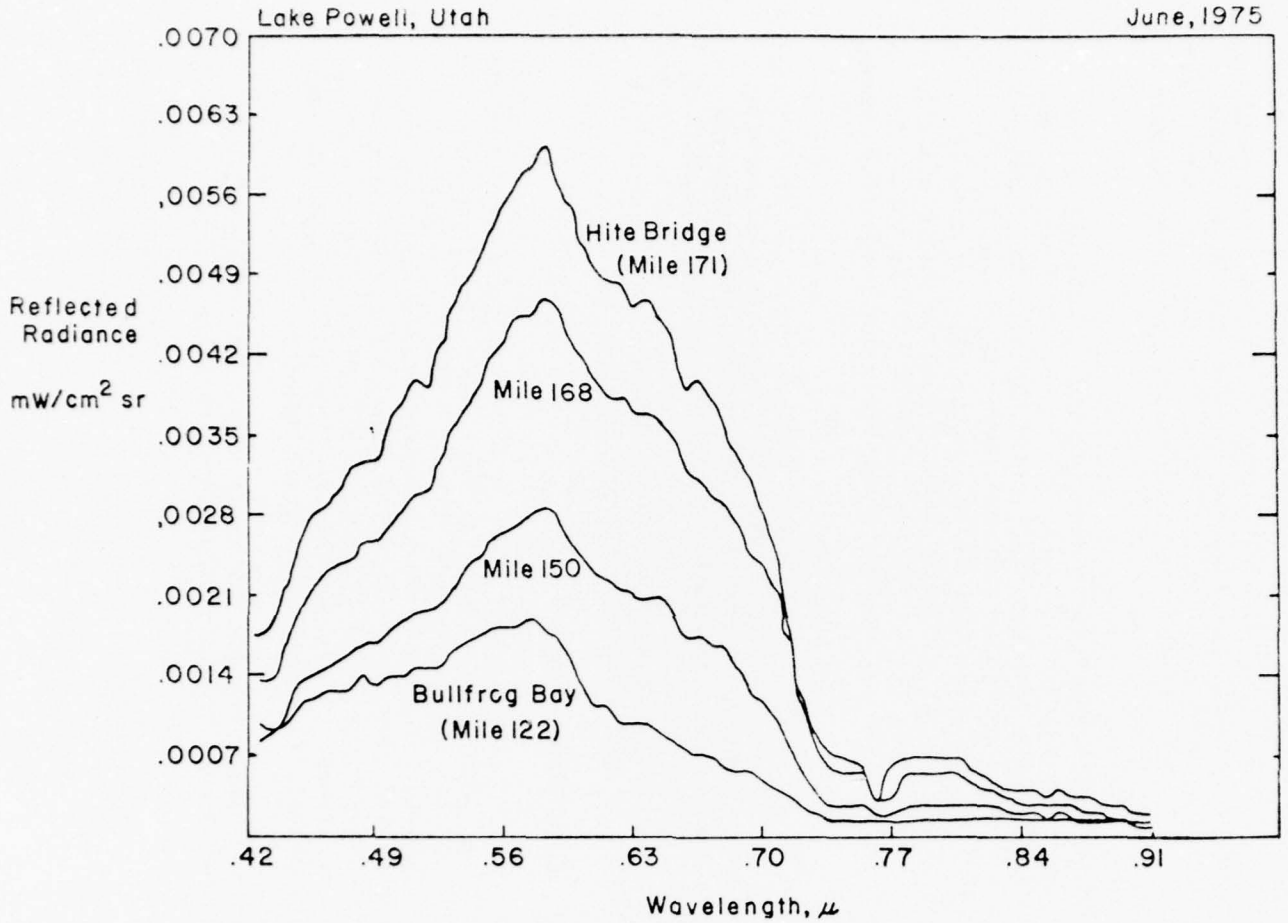

Figure 6. Airborne spectroradiometer data of selected locations in Lake Powell, Utah (June 1975).

The spectral data are shown with wavelength in microns (μ plotted along the x-axis and reflected radiance in mW/cm^2 sr along the y-axis. The wavelength channel width of the aircraft spectroradiometer data used in this analysis was 14.96Å and, therefore, the reflected radiance can be expressed as mW/cm^2 sr-channel. However, throughout the remainder of this report the reflected radiance will be expressed in mW/cm^2 sr with the channel width assumed to be 14.96Å.

A typical spectrum is composed of 500 individual data points or 500 channels of approximately 14Å width. These reflected radiance values cover a total spectral region from 0.42μ to approximately 0.90μ. The spectral regions represented by the aircraft spectra are located in the visible wavelength region from 0.4-0.7μ and the near infrared region from 0.7-1.5μ. The sharp drops in the spectral curves are due to various absorption bands caused by the presence of water vapor and oxygen in the atmosphere and, to a lesser extent, the presence of Fraunhofer lines in the solar incident radiation. For example, a water absorption band occurs at 0.76μ (Hodgman et al., 1953).

The range of reflected radiance values in the Bullfrog Bay (Mile 122) water spectrum was low when compared with the Hite Bridge (Mile 171), Mile 168 and Mile 150 spectra throughout the entire 0.42 to 0.91μ wavelength region (Fig. 6). The percentage of transmittance at Bullfrog Bay (Mile 122) was high (95.4%) which indicated that the water had a very low turbidity (Table III). This was verified by the secchi disk depth measurement of 4.5 m (Table II) which was the deepest depth of light extinction in Lake Powell that was obtained from all the water samples (Fig.5). Initially, the reflected radiance value was 0.0010 mW/cm^2 sr at an initial sampling wavelength of 0.42μ, but increased to a broad peak of 0.0017 mW/cm^2 sr centered at 0.58μ. The reflected radiance values then gradually decreased to a value of 0.0001 mW/cm^2 sr at 0.76μ.

The Mile 150 aircraft spectrum was somewhat different in appearance from the Bullfrog Bay (Mile 122) spectrum (Fig. 6). The initial reflected radiance value was 0.0008 mW/cm^2 sr at a wavelength of 0.42μ and increased to 0.0027 mW/cm^2 sr at a wavelength of 0.58μ. A secondary spectral shoulder occurred at 0.64μ at a reflected radiance value of 0.0017 mW/cm^2 sr. Secchi disk depth measurements showed a 3.75 m decrease in depth penetration from Bullfrog Bay (Mile 122) to Mile 150 (Table II). The percentage of light transmittance had decreased to a value of 89.7% in the Mile 150 sample (Table III). The Mile 150 spectrum in contrast to the Bullfrog Bay (Mile 122) spectrum showed higher reflected radiance values in the near infrared region (0.70-0.91μ) indicating that the Mile 150 sample contained more turbidity than that observed at Bullfrog Bay (Mile 122).

The Mile 168 spectrum was similar in shape to the Mile 150 spectrum; however, the entire curve had increased to higher reflected radiance values (Fig. 6). The turbidity in the Mile 169 water sample had also

increased and is indicated by a lower value of percentage transmittance (64.1%) and a lower secchi disk depth measurement (0.30 m) than occurred in the Mile 150 or Bullfrog Bay (Mile 122) samples (Tables II, III). Also, as in the Bullfrog Bay (Mile 122) and Mile 150 spectrum, the peak in reflected radiance value occurred at 0.58μ (Fig. 6). In addition, a secondary spectral shoulder occurred at 0.64μ similar to the Mile 150 spectrum.

The greatest amount of turbidity was measured in the Hite Bridge (Mile 171) water sample. The percentage of light transmittance measured in the laboratory was 39.2% and the secchi disk depth measured 0.18 m (Tables II, III). The reflected radiance value observed at the 0.42μ wavelength (0.0017 mW/cm^2 sr) was larger than observed in the other three samples and increased to 0.0060 mW/cm^2 sr at a wavelength of 0.58μ (Fig. 6). In the 0.58-0.91μ range the reflected radiance value decreased rapidly to a value of 0.0007 mW/cm^2 sr with a secondary spectral shoulder occurring at 0.64μ (0.0046 mW/cm^2 sr). In the 0.76-0.91μ wavelength region the reflected radiance was relatively greater in intensity (0.0007 mW/cm^2 sr) for the Hite Bridge (Mile 171) area compared to the other spectra. In the near infrared region the light does not penetrate deep within the water. If the surface water has very low turbidity the reflected light will be low and, therefore, the reflected radiance is very low. If large quantities of particulates occur in the surface water (high turbidity), the reflection becomes greater and the corresponding reflected radiance value will increase.

From these data it is possible to correlate the turbidity in the water samples to the spectra obtained from the airborne spectroradiometer instrument. It can be stated that as the turbidity in the water increases the spectral reflected radiance curve increases throughout the 0.42-0.91μ wavelength region with the peak reflected radiance value occurring at 0.58μ. Also, a secondary spectral shoulder occurred at 0.64μ for the Mile 150, Mile 168 and Hite Bridge (Mile 171) spectra, but this shoulder was absent for the Bullfrog Bay (Mile 122) spectrum.

Analysis of particulate matter

The concentration of particulate matter in the water samples was determined by the filtration procedure described previously (Table V). These concentrations contributed to the turbidity of the water samples.

Table V. Concentration data from selected Lake Powell water samples (June 1975).

Location	Concentration (filtered) (mg/l)
Hite Bridge (Mile 171)	77.2
Mile 168	41.1
Mile 150	5.9
Bullfrog Bay (Mile 122)	4.9

The electron micrographs obtained of the water samples show the differences in the composition of the particulate matter. Figure 7a illustrates the low concentration of particulate matter in the Bullfrog Bay (Mile 122) water and Figure 7b shows the resulting precipitated salt crystals after evaporation of the water sample. Figure 8a, b, c show clay and other inorganic materials that increase in concentration from Mile 150 to Mile 168 to Hite Bridge (Mile 171). The insoluble inorganics composing the major portion of the particulate matter in these samples are probably clay minerals or clay-sized particles.

Runoff from the surrounding areas carry particles of both clay minerals and clay-sized materials. Very little organic matter enters Lake Powell from the land. The principal clay minerals found in the area are illite, montmorillonite and kaolinite (Mayer, 1973). Also, carbonaceous materials occur throughout the river basin.

By examining the enlarged photographs of the water samples (Figs. 7 and 8) an inference of the type of particulate matter in the water can be obtained. The Hite Bridge (Mile 171), Mile 168 and Mile 150 water samples comprised mainly clay materials as evidenced by platy and irregular particle shapes. The Bullfrog Bay (Mile 122) water sample contained very little particulate matter with predominantly salts present.

A comparison of the ground truth measurements for the Hite Bridge (Mile 171), Mile 168 and Mile 150 water samples showed the following trends:

1. The percentage of transmittance measured in the field and laboratory increased from Hite Bridge (Mile 171) to Mile 168 to Mile 150.

2. The secchi disk depth measurement increased from Hite Bridge (Mile 171) to Mile 168 to Mile 150.

3. The concentration determined by filtration decreased from Hite Bridge (Mile 171) to Mile 168 to Mile 150.

When comparing the data obtained for the Bullfrog Bay (Mile 122) area to the trends observed for the other three sites, the following observations were made:

1. The percentage of transmittance measured in the field and laboratory increased in value from Mile 150 to Bullfrog Bay (Mile 122).

2. The secchi disk depth data increased in value from Mile 150 to Bullfrog Bay (Mile 122).

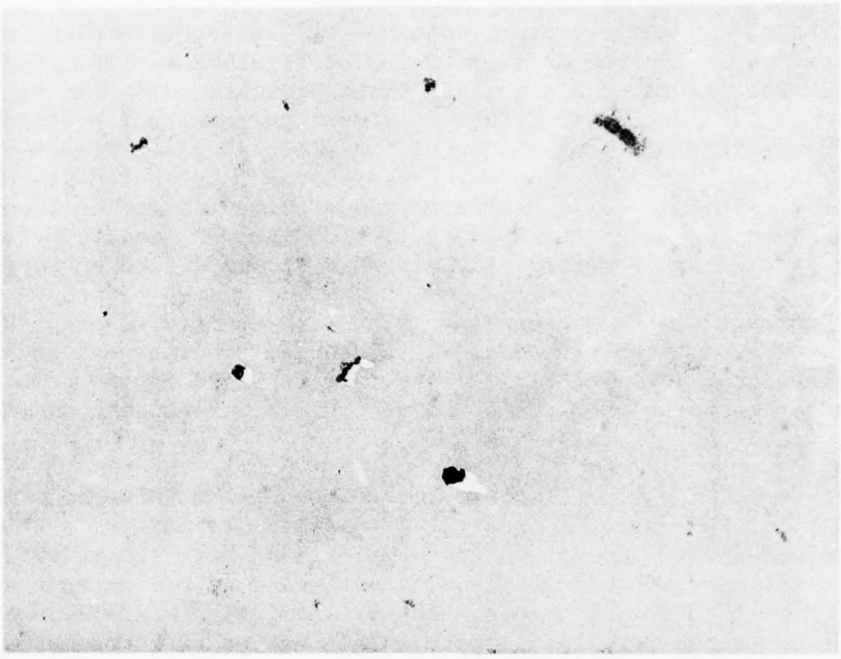

a. Electron micrograph (3675x enlargement).

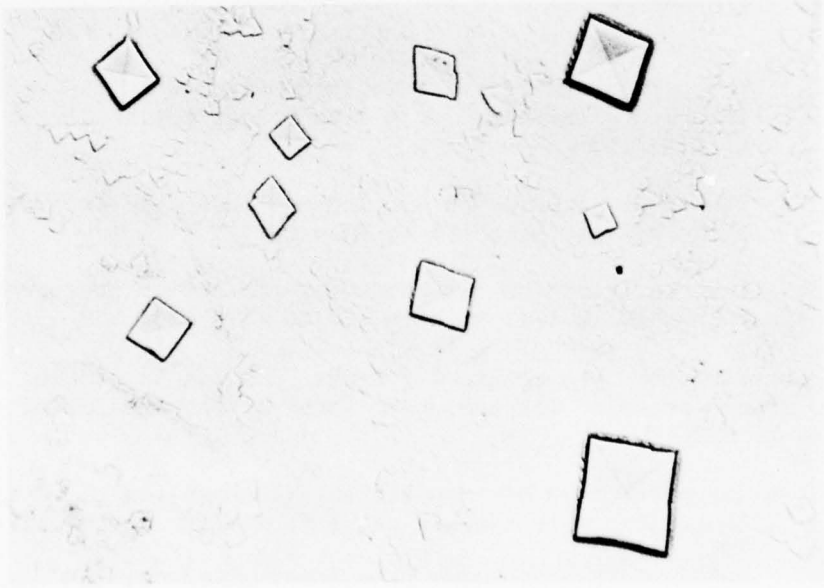

b. Photograph showing precipitated salts (72x enlargement).

Figure 7. Photographs of the Bullfrog Bay (Mile 122) water sample.

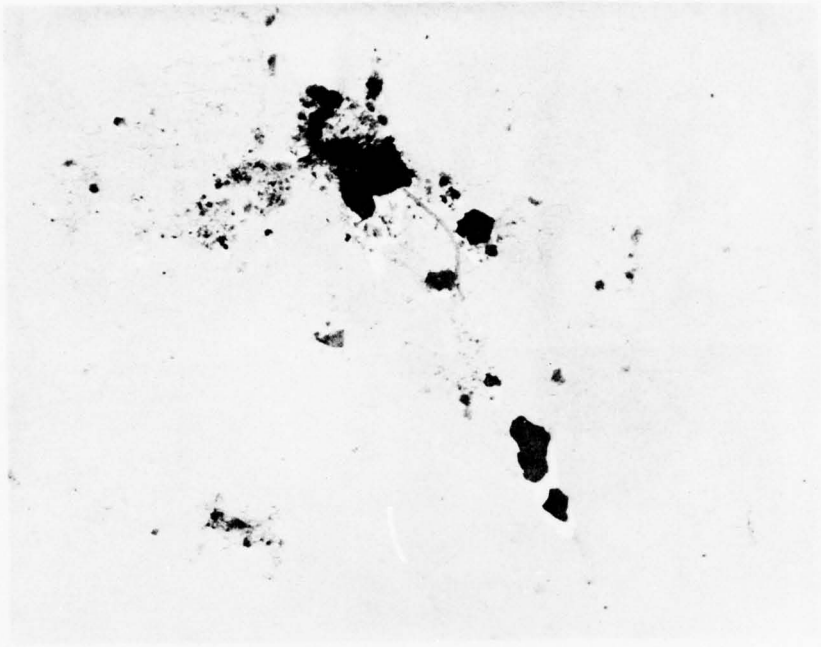

a. Mile 150.

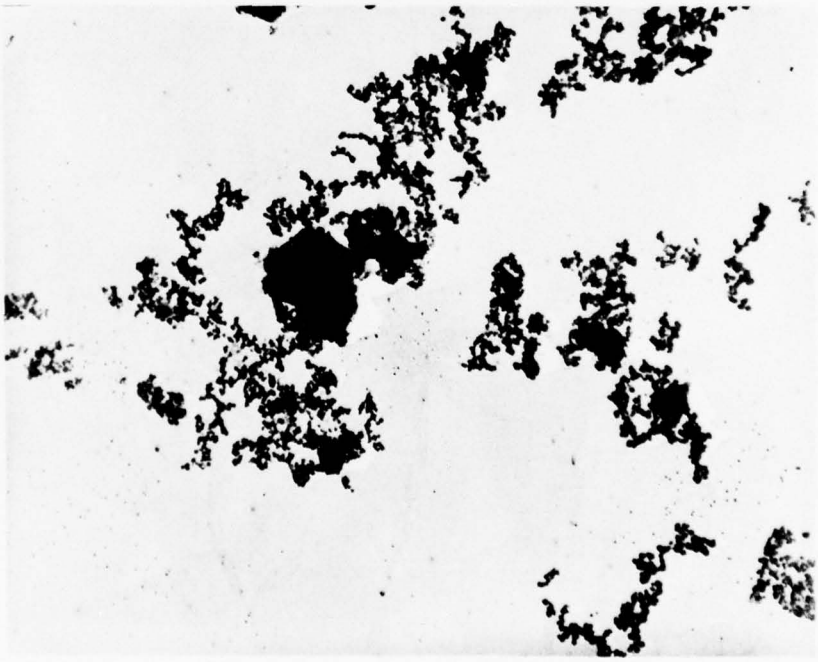

b. Mile 168.

Figure 8. Electron micrographs of selected Lake Powell water samples (3675x enlargement).

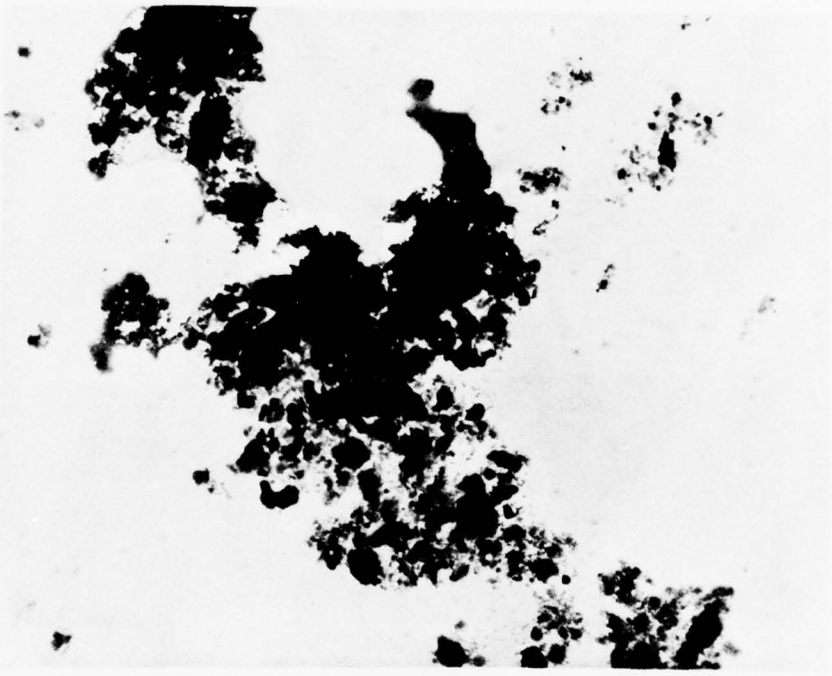

c. Hite Bridge (Mile 171).

Figure 8. Electron micrographs of selected Lake Powell water samples (3675x enlargement).

3. The concentration determined by filtration decreased from 5.9 mg/l in the Mile 150 area to 4.9 mg/l in the Bullfrog Bay area (Mile 122); however, the concentration differed by only 1 mg/l.

In summary, the Bullfrog Bay (Mile 122) and Mile 150 area showed about the same relative particulate concentration, but this similarity in concentration was not reflected by a similar aircraft spectrum curve. It can be seen in Figure 6 that the Mile 150 aircraft spectrum had a larger overall reflected radiance than the Bullfrog Bay (Mile 122) spectrum. Also, the spectral shoulder at 0.64μ, which was present in the Mile 150, Mile 168 and Hite Bridge (Mile 171) spectra, was absent in the Bullfrog Bay (Mile 122) spectrum.

The concentrations determined by the filtration method (Table V) for the four test sites are compared against the reflected radiance value in Figure 9 for the wavelengths of 0.58μ and 0.64μ, selected because of the prominent spectral features--a peak at 0.58μ and shoulder at 0.64μ. Also, the reflected radiance value at 0.79μ was plotted against the concentration to give representative data in the near infrared region. In all cases the measurements for the Bullfrog Bay (Mile 122) water fell outside the curves fitted between the Mile 150, Mile 168 and Hite Bridge (Mile 171) data.

This feature of the aircraft spectra suggested that the particulate matter in the Bullfrog Bay (Mile 122) water may be significantly different than the other three sites. On examining the location of the test sites (Fig. 3) it can be seen that Bullfrog Bay is a large tributary off of the main Colorado River channel. The water in Bullfrog Bay was a year old in June 1975 and should not be compared to the other three sites located on the main Colorado River channel. In addition, the chemistry, mineralogy and particle distribution of the Bullfrog Bay water has an unknown relationship to the water conditions in the main channel. Also, the Bullfrog Bay tributary has a different drainage area than the other three sites and thus would be receiving different sediment inputs from the land.

The surface waters of Lake Powell are characterized mainly by sulfates, carbonates and chlorides (Reynolds and Johnson, 1974). The concentration of the carbonate increases downstream from Hite Bridge and the water becomes oversaturated with carbonate as the salinity (Table VI)

Table VI. Salinity of selected Lake Powell water samples (June 1975).

Location	Conductivity (mmhos)	Est. NaCl (mg/l)
Hite Bridge (Mile 171)	0.40	180
Mile 168	0.44	198
Mile 150	0.50	225
Bullfrog Bay (Mile 122)	0.56	250

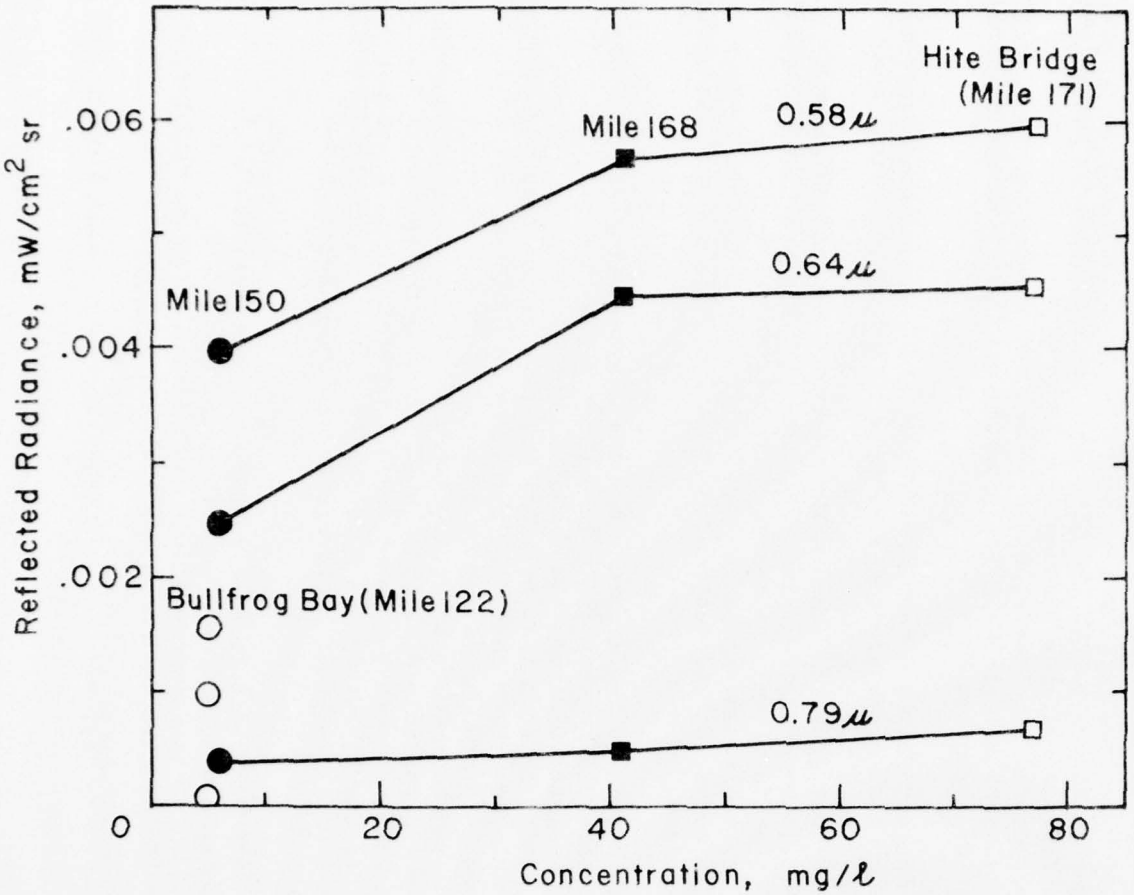

Figure 9. Graph illustrating concentration in mg/l vs. reflected radiance for wavelengths of 0.58μ, 0.64μ and 0.79μ. All points are normalized to a sun angle elevation of 42.7 degrees.

and temperature in Lake Powell (Table II) increase downstream (Reynolds, 1976). Also, during June 1975 the sediment load was at a maximum at the Hite Bridge area (Mile 171) due to spring runoff conditions and the turbidity decreased downstream.

It is suggested that the carbonates and siliceous materials reflect differently in the visible spectrum and this mixture of two kinds of particulate matter is the cause of the two spectral features--the 0.58μ peak and the shoulder at 0.64μ--that were observed in the aircraft spectra. The Bullfrog Bay (Mile 122) water is greener to the eye, suggesting the greater carbonate content. Also, the salinity and temperature were the highest in the Bullfrog Bay area water suggesting a greater carbonate content (Reynolds, 1976). Therefore, the spectral peak at 0.58μ may be associated with the carbonate or green peak in the spectral curve.

The spectral curve at 0.64μ is absent in the Bullfrog Bay (Mile 122) sample. The explanation for this is probably the fact that very little siliceous particulate matter or sediment is present in Bullfrog Bay (Mile 122). The remaining three water samples are composed of both the carbonate and siliceous particulate matter and, therefore, the spectral curves show both a spectral peak at 0.58μ and shoulder at 0.64μ.

Comparison with the theoretical model

To obtain quantitative information from the aircraft spectra, spectral data at the key wavelengths of 0.58μ and 0.64μ were compared with results from a theoretical calculation of water spectra carried out at the NASA GISS by Travis and Hansen (1976). For this comparison they had to assume a gelbstoff component (Kalle, 1966) in addition to siliceous particles to match the shape and magnitude of the aircraft spectral curves (Travis and Hansen, 1976).

The particle size and particle concentration, determined by scanning electron microscopy (EMV Associates, 1976) and by filtration, were also used in the theoretical model. In addition, the model assumed a particle refractive index of 1.2 that is suitable for clay materials according to standard textbooks (Kerr, 1959; Kraus et al., 1959). The absorption coefficient of the particles, which was unknown, was adjusted by Travis and Hansen to secure agreement with the aircraft observations at Hite Bridge (Mile 171).

The results, shown in Figure 10a and 10b, indicate major disagreements between the aircraft measurements and the theoretical model, in both shape and magnitude of the curves, for reflected radiance intensity vs. concentration. The agreement at Hite Bridge (Mile 171) is due to adjustment of the absorption coefficient, as indicated above, and is not significant. If a third component consisting of calcite particles were assumed in the model, in addition to siliceous and gelbstoff components,

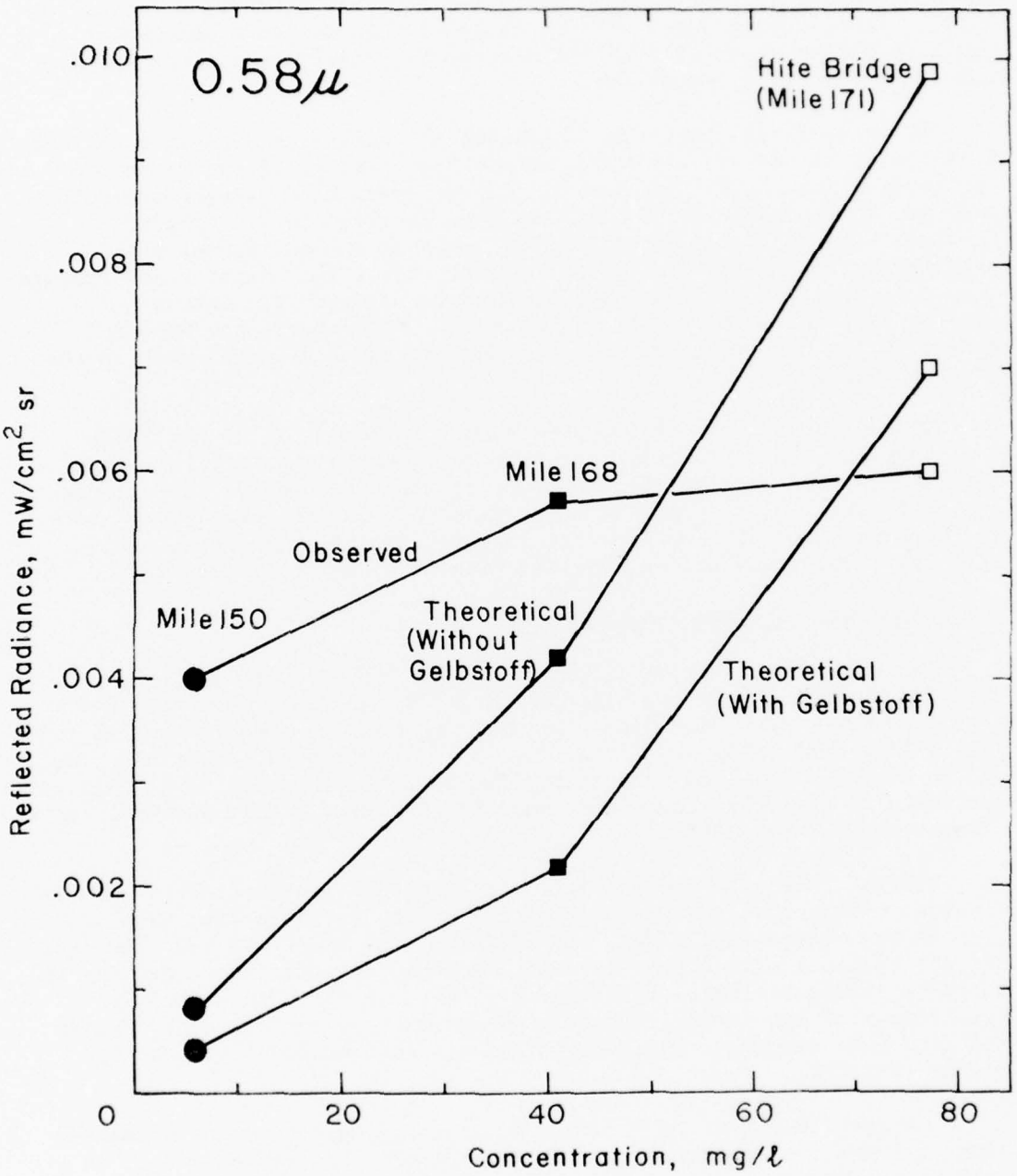

a. Comparison at 0.58μ.

Figure 10. Comparison of aircraft measurements to the theoretical model. All points have been normalized to a sun angle elevation of 42.7 degrees.

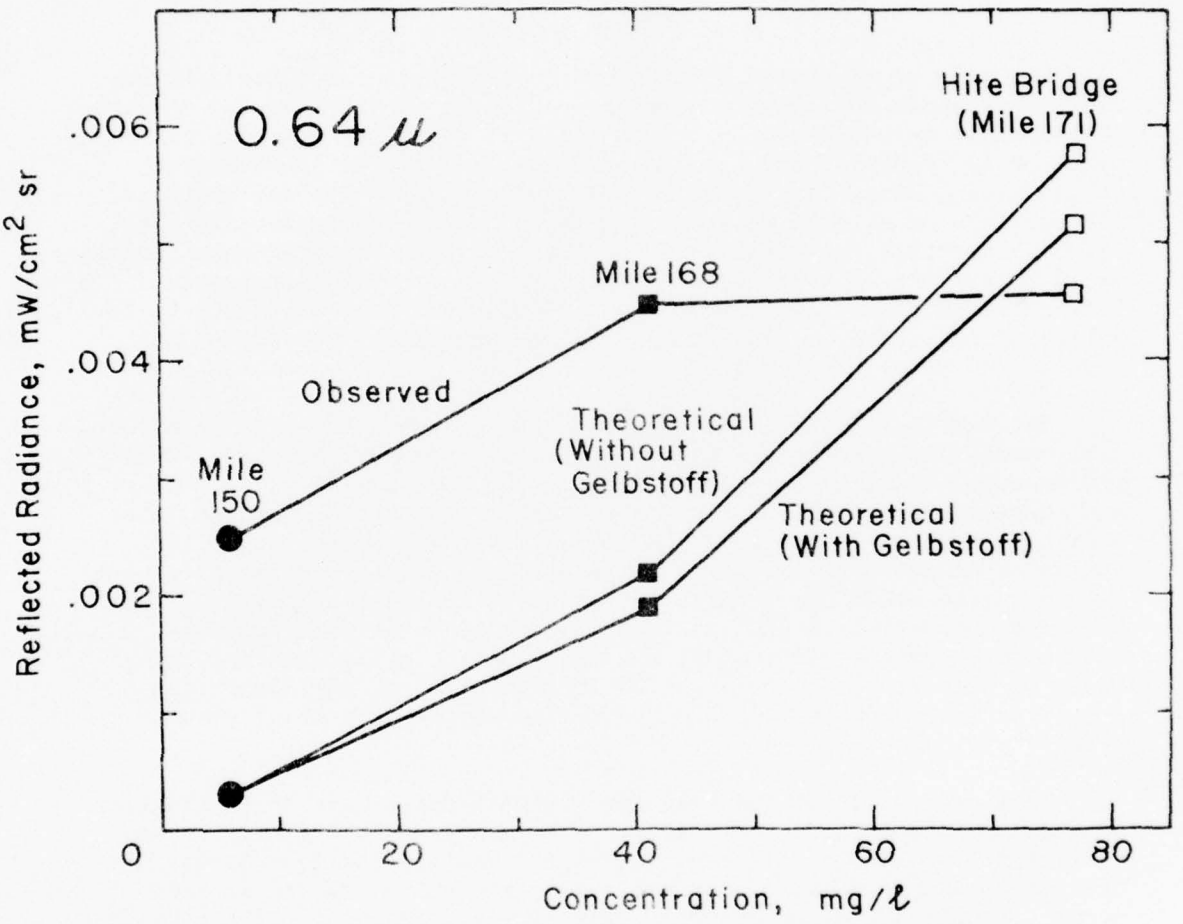

b. Comparison at 0.64μ.

Figure 10. Comparison of aircraft measurements to the theoretical model. All points have been normalized to a sun angle elevation of 42.7 degrees.

a closer fit between the theoretical and aircraft spectra could be obtained. However, little or no information would result from this agreement because the number of adjustable parameters would be at least as great as the number of data points. In any case, a simple theoretical model in which the major component consists of siliceous clay particles cannot describe the aircraft spectral measurements.

CONCLUSIONS

Analysis of the water spectra obtained from the airborne spectroradiometer shows that remote sensing techniques can be a useful measure of turbidity in water bodies. Valuable *qualitative* information can be obtained by comparing the Lake Powell water spectra to spectra from other water bodies. The spectral peak centered at 0.58μ may indicate the presence of calcite which is a measure of lake salinity (Reynolds, 1976). Therefore, detection of this spectral peak in other water bodies would be a means of classifying lakes (hard and soft) using remote sensing techniques. Also, the shoulder at 0.64μ is probably due to the siliceous particles and can be taken as a qualitative measure of the presence of these particles.

The remote sensing technique also shows promise of being an effective *quantitative* method. The quantification consists in correlating the measured spectral reflected radiance, at some key wavelength or wavelengths, with the measured concentration of particles in the water. Ideally, the correlation could be tested by measuring the reflected radiances at one site in the lake and at several different times of the year when the water has a different particle content. A graph of the particle concentration *vs.* the reflected radiance at some suitably chosen wavelength would then give a quantitative relationship that could be used to determine particle concentration at any other time solely by the measurement of the reflected radiances without ground truth verification.

This project permitted only one aircraft flight and an examination of measurements at different times of the year over the same site was not feasible. However, some pertinent information could be obtained from the measurements taken at the same time, but at different sites along the Colorado River channel. The aircraft measurements are shown in Figure 10 and display the same major spectral features--a peak at 0.58μ and a shoulder at 0.64μ--for three sites, namely Hite Bridge (Mile 171), Mile 168 and Mile 150. This suggests (although it does not prove) that the particle content and mineralogy are similar at the three sites. Therefore, the particle concentration vs. reflected radiance was plotted for key wavelengths (chosen as 0.58μ, 0.64μ and 0.79μ) and these graphs can be used as the quantitative measure of particle content in this reach of the Colorado River channel as determined by remote sensing techniques.

The relationship implied in Figure 9 should be tested for uniqueness and reproducibility to complete the study of the quantitative usefulness of reflected radiances in monitoring of water quality. Such tests will require additional flights at different times of the year and also over different lakes. The results obtained in the present investigation are sufficiently encouraging to justify such flights, if resources can be made available.

One other useful line of research for the future would be measurements under controlled conditions, in laboratory tank tests if feasible, and if not, then in carefully selected bodies of water in the field. If tank tests are feasible, known concentrations of various types of particulate matter could be dispersed in water tanks and spectra could be obtained using the airborne spectroradiometer. Physical properties of the particulate matter, such as particle size, number and distribution and optical properties of the particles, would be previously determined. The relationship of these parameters to the shape and intensity of the water spectra could then be analyzed and also compared with results from theoretical models of the scattering of radiation penetrating through turbid water. This combination of theoretical work and laboratory or controlled field experiments would provide a solid foundation for further development of remote sensing as a practical tool in the monitoring of water quality.

LITERATURE CITED

Blackwell, R.J. and D.H. Boland (1973) The Trophic Classification of Lakes Using ERTS Multispectral Scanner Data, Research Paper Results, NASA Contract no. NAS7-100, 21 p.

Blanchard, B.J. and R.W. Leamer (1973) Spectral Reflectance of Water Containing Suspended Sediment, Remote Sensing and Water Resources Management, Proc. no. 17, American Water Resources Association, p. 339-347.

Bowker, D.E., P. Fleischer, T.A. Gosink, W.J. Hanna and J. Ludwick (1973) Correlation of ERTS Multispectral Imagery with Suspended Matter and Chlorophyll in Lower Chesapeake Bay, Symposium on Significant Results obtained from ERTS-1 (5-9 March), NASA Goddard Space Flight Center, Greenbelt, Maryland, NASA SP-327, p. 1291-1297.

Coleman Instruments (1969) Coleman Model 14 Universal Spectrophotometer, 14-900 Operating Directions, Coleman Instruments: Maywood, Illinois, p. 18-29.

Collins, W. (1976) Spectroradiometric Detection and Mapping of Areas Enriched in Ferric Iron Minerals using Airborne and Orbiting Instruments, PhD thesis, Columbia University, New York, New York, 120 p.

Defant, A. (1961) *Physical Oceanography*, Pergamon Press: New York, New York, p. 51-64.

Egan, W.G. (1972) Water Quality Determinations in the Virgin Islands from ERTS-A data, Proceedings of the Eighth International Symposium on Remote Sensing of Environment (2-6 October), ERIM, University of Michigan, Ann Arbor, Michigan, p. 685-708.

Egan, W.G. (1974) Boundaries of ERTS and Aircraft Data within which Useful Water Quality Information can be Obtained, Proceedings of the Ninth Symposium on Remote Sensing of Environment (15-19 April), ERIM, University of Michigan, Ann Arbor, Michigan, p. 1319-1344.

EMV Associates, Inc. (1976) Personal communication.

Gramms, L.C. and W.C. Boyle (1971) Reflectance and Transmittance Characteristics of Selected Green and Blue-green Unialgae, Center for Environmental Communications and Education Studies - University of Wisconsin Remote Sensing Program, Report no. 5, 25 p.

Grew, G.W. (1973) Signature Analysis of Reflectance Spectra of Phytoplankton and Sediment in Inland Waters, Remote Sensing of Earth Resources, Vol. II, Benson Printing Company: Nashville, Tennessee, p. 1147-1172.

Hansen, J.E. (1976) Personal communication.

Hodgman, C.D., R.C. Weast and C.W. Wallace (editors) (1953) Handbook of Chemistry and Physics, Thirty-fifth Edition, Chemical Rubber Publishing Company: Cleveland, Ohio, 3163 p.

Hutchinson, G.E. (1957) A Treatise on Limnology, Vol. 1, John Wiley and Sons, Inc.: New York, New York, 1015 p.

Jarrett, O., Jr., P.B. Mumola and C.A. Brown, Jr. (1973) Four Wavelength Lidar Applied to Determination of Chlorophyll *a* Concentration and Algae Color Group, Remote Sensing and Water Resources Management, Proc. no. 17, American Water Resources Association, p. 259-268.

Jerlov, N.G. (1968) Optical Oceanography, Vol. 5, Elsevier Publishing Company: New York, New York, 194 p.

Jerlov, N.G. (ed.) (1974) Optical Aspects of Oceanography, Academic Press: New York, New York, 494 p.

Johnson, N.M. and D. Merritt (1975) Personal communication.

Kalle, K. (1966) The Problem of the Gelbstoff in the Sea, Oceanography Marine Biol. Ann. Rev., Vol. 4, p. 91-104.

Kerr, P.F. (1959) Optical Mineralogy, McGraw-Hill Book Company: New York, New York, 442 p.

Klemas, V., D. Bartlett, W. Philpot, R. Rogers and L. Reed (1974) Coastal and Estuarine Studies with ERTS-1 and Skylab, Remote Sensing of Environment, Vol. 3, p. 153-174.

Klemas, V., J.R. Borchardt and W.M. Treasure (1973) Suspended Sediment Observations from ERTS-1, Remote Sensing of Environment, Vol. 2, p. 205-221.

Kraus, E.H., W.F. Hunt and L.S. Ramsdell (1959) Mineralogy, McGraw-Hill Book Company: New York, New York, 686 p.

Kritikos, H., L. Yorinks and H. Smith (1974) Suspended Solids Analysis Using ERTS-A Data, Remote Sensing of Environment, Vol. 3, p. 69-78.

Kumai, M. (1976) Personal communication.

Lacis, A.A., D.L. Coffeen, J.E. Hansen, S. Lebedeff, T. Mo and L.D. Travis (1976) Experiment Proposal, Photopolarimeter for Ocean and Lake Applications (AQUAPOL), 57 p.

Maul, G.A. and H.R. Gordon (1973) Relationships between ERTS Radiances and Gradients across Oceanic Fronts, Third Earth Resources Technology Satellite-1 Symposium (10-14 December), NASA Goddard Space Flight Center, Greenbelt, Maryland, NASA SP-351, p. 1279-1308.

Maul, G.A. and H.R. Gordon (1975) On the Use of the Earth Resources Technology Satellite (LANDSAT-1) in Optical Oceanography, Remote Sensing of Environment, Vol. 4, p. 95-128.

Mayer, L. (1973) Aluminosilicate Sedimentation in Lake Powell, Master's thesis, Dartmouth College, Hanover, New Hampshire.

Mie, G. (1908) Beiträge zur Optick Trüber Medien, Speziell Kolloidalen Metalllösungen, Ann. Physik, Vol. 25, p. 377.

NASA (1971) Earth Resources Technology Satellite Data User's Handbook, NASA Document no. 71SD4249.

NOAA (1975) Climatological Data - June 1975, Environmental Data Service: Asheville, North Carolina, Vol. 77, no. 6, 25 p.

Polcyn, F.C. and Lyzenga, D.R. (1973) Multispectral Sensing of Water Parameters, Remote Sensing and Water Resources Management, Proc. no. 17, American Water Resources Association, p. 394-403.

Rayleigh, Lord (1871) On the Scattering of Light by Small Particles, Phil. Mag., Vol. 41, p. 447-454.

Reynolds, R.C. (1976) Personal communication.

Reynolds, R.C. and N.M. Johnson (1974) Major Element Geochemistry of Lake Powell, Lake Powell Research Project Bulletin, no. 5, National Science Foundation, 14 p.

Rogers, R.H., L.E. Reed and V.E. Smith (1975) Computer Mapping of Turbidity and Circulation Patterns in Saginaw Bay, Michigan, from LANDSAT Data, Special Report no. E75-10321, NASA Contract no. NAS5-20942, 16 p.

Scherz, J.P., M. Sydor and J.R. Van Domelen (1973) Aircraft and Satellite Monitoring of Water Quality in Lake Superior Near Duluth, Third Earth Resources Technology Satellite-1 Symposium (10-14 December), NASA Goddard Space Flight Center, Greenbelt, Maryland, NASA SP-351, p. 1619-1636.

Smoluchowski, M. (1908) Molekular-kinetische Theorie der Opaleszenz von Gasen im Kritischen Zustande, Sowie Einiger Verwandter Erscheinungen, Ann. Physik, Vol. 25, p. 205.

Strong, A.E. (1974) Remote Sensing of Algal Blooms by Aircraft and Satellite in Lake Erie and Utah Lake, Remote Sensing of Environment, Vol. 3, p. 99-107.

Travis, L.D. and J.E. Hansen (1976) Personal communication.

Williamson, A.N. and W.E. Grabau (1973) Sediment Concentration Mapping in Tidal Estuaries, Third Earth Resources Technology Satellite-1 Symposium (10-14 December), NASA Goddard Space Flight Center, Greenbelt, Maryland, NASA SP-351, p. 1347-1386.

Wrigley, R.C. and A.J. Horne (1974) Remote Sensing and Lake Eutrophication, Nature, Vol. 250, p. 213-214.

Yarger, H.L., J.R. McCauley, G.W. James, L.M. Magnuson and G.R. Marzolf (1973) Water Turbidity Detection Using ERTS-1 Imagery, Symposium on Significant Results Obtained from ERTS-1 (5-9 March), NASA Goddard Space Flight Center, Greenbelt, Maryland, NASA SP-327, p. 651-653.

APPENDIX A

LITERATURE REVIEW

Optical properties of water

Considerable research in the past ten years has resulted in numerous articles on the optical properties of water. A significant contribution was presented in which the definitions for attenuation, absorption and scattering were mathematically stated as the following relation (Jerlov, 1974):

$$c = a + b \tag{1}$$

$$b = 2\pi \int_0^{\pi} \beta(\theta) \sin\theta \, d\theta \tag{2}$$

where: c = attenuation coefficient
a = absorption coefficient
b = total scattering coefficient
$\beta(\theta)$ = volume scattering function

It is evident from equation (1) that attenuation of water is derived from both scattering and absorption. Absorption has often been used instead of attenuation because scattering is negligible compared to absorption in the total wavelength spectrum, except in the 0.4-0.5μ spectral region where the absorption or attenuation coefficient is minimal (Jerlov, 1974).

The scattering of light in turbid water is primarily caused by reflection and diffraction of the incident light by suspended particles in the water (Jerlov, 1968). The simplest scattering occurs at low concentrations when the size of the suspended particles is small compared to the measured wavelength. The scattering of light is due to diffraction and follows Rayleigh's law (Rayleigh, 1871) which states that the reduction in the intensity of the incident light is inversely proportional to the fourth power of the wavelength (λ^{-4}).

The Tyndall effect occurs when a beam of light passing through turbid water illuminates the suspended particles. The illumination is caused by reflection and scattering of the incident light. The Tyndall light is bluish in color at shorter wavelengths because light at these wavelengths is strongly scattered. This phenomenon has been used to explain the blue color of scattered light in pure water since the water molecules were the scattering particles.

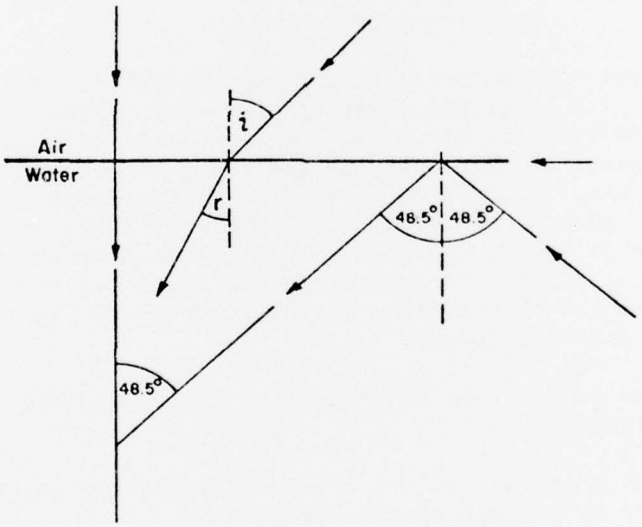

Figure A1. Schematic diagram illustrating refraction and total reflection.

Subsequently, it was found that direct scattering of the water molecules could not occur because the water molecules were compressed and the distance between the molecules was very small relative to the diameter (Defant, 1961). Later, the fluctuation theory (Smoluchowski, 1908) stated that irregular molecular movements gave rise to an optical inhomogeneity (or Schlieren streaks of very small dimensions) which was responsible for the scattering of light.

Parallel light rays incident on a water surface will in part be reflected and in part enter the water (Fig. A1). The angle of reflection will equal the angle of incidence, but the ratio of the intensities of the incident and reflected light will be dependent on the angle of incidence which can vary between 0-90°. Light which enters the water will change direction on passing through the water surface and the angle of the refracted beam is represented by the following equation (Snell's Law):

$$\frac{\sin i}{\sin r} = n$$

where: i = angle of incidence
r = angle of reflection
n = refractive index

For air and pure water, n will be approximately equal to 4/3 (Jerlov, 1968). A light ray striking the water surface vertically from below continues into the air along the same path. If the path deviates from the vertical, the light ray is refracted from the perpendicular at the surface. When an angle of 48.5° from the vertical is reached, the light ray will pass along the surface. For any angle greater than the critical angle of 48.5°, the light is reflected downward and, therefore, the 48.5° is called the critical angle for total reflection. The critical angle is determined by the ratio of the velocity of light in the two mediums (or refractive index).

Scattering of light is the result of three physical phenomena which are (Jerlov, 1968):

1) light that is deviated from rectilinear propagation (diffraction) by the action of a particle.

2) light that will penetrate a particle and emerge with or without one or more internal reflections (refraction).

3) light that is only reflected externally (reflection).

Particle size is the major component of light scattering. For large particles the scattering is almost independent of the wavelength and depends primarily on that part of the total surface area of the particle influenced by the light. Therefore, scattering by large particles is not

color selective. Diffraction will occur independent of the particle's composition, whereas refraction and reflection are determined by the refractive index of the particle (Jerlov, 1968).

In contrast to Rayleigh scattering, the Mie theory of scattering occurs for a model system composed of particles with a given refractive index and pure water (Mie, 1908). Also, the scattered light has the same wavelength as the incident light. In this theory the particles are spherical and larger than those assumed for Rayleigh scattering with the distance between the spheres being at least three times the radius. Also, multiple scattering does not occur. Therefore, the total scattering is proportional to the number of particles.

Correlation of multispectral data to water quality

Numerous investigators have studied the problem of correlating spectral measurements with suspended sediment and algal concentrations (Blanchard and Leamer, 1973; Bowker et al., 1973; Gramms and Boyle, 1971; Grew, 1973; Jarrett et al., 1973; Maul and Gordon, 1973, 1975; Polycyn and Lyzenga, 1973; Wrigley and Horne, 1974). Generally, these experiments utilize a ratioing technique between broad spectral bands in the 0.5-1.1μ region. This is accomplished to measure and distinguish between suspended sediment and algae concentrations and surface areal distribution which is a qualitative measure of turbidity. It is difficult to obtain quantitative information on materials in the water because the color measurements of the observed radiance result from a combination of surface reflection, atmospheric scattering and light scattering within the water body (Lacis et al., 1976). Techniques which can separate the contributions to the observed radiances from these different mechanisms would be useful for improving remote sensing capabilities (Lacis et al., 1976).

In addition to aircraft sensors, satellite sensors have been used to monitor water quality. One of the latest sensor developments has been the multispectral scanner (MSS) aboard Landsat, a polar orbiting satellite. The multispectral scanner comprises four channels; MSS 4 (0.5-0.6μ), MSS 5 (0.6-0.7μ), MSS 6 (0.7-0.8μ) and MSS 7 (0.8-1.1μ). The ground coverage of a Landsat scene is 100 nautical miles on a side (185 km) with a pixel resolution of 1.1 acres (57x79 m). The satellite orbits the earth in 103 minutes, completing 14 orbits a day. Coverage of a given area occurs every 18 days at the same local time. The multispectral data are quantized onboard the satellite (128 gray levels for MSS 4, 5, 6; 64 for MSS 7) and relayed in a digital bit stream to a ground receiving station. An oscillating mirror system reflects upwelling radiation from the earth into six detectors for each channel so that six scan lines are observed simultaneously (NASA, 1971).

Published results indicate that for Landsat MSS band 5 (0.6-0.7μ) high densities of suspended sediment correspond to high water reflectance

and low densities correspond to low water reflectance; therefore, gross sediment and circulation patterns can be delineated for large water bodies (Blackwell and Boland, 1973; Egan, 1972, 1974; Klemas et al., 1973, 1974; Kritikos et al., 1974; Rogers et al., 1975; Scherz et al., 1973; Strong, 1974; Williamson and Grabau, 1973; Yarger et al., 1973). Again, only qualitative information has been derived from these Landsat multispectral analyses.

APPENDIX B

WATER QUALITY DATA OF LAKE POWELL

WATER SAMPLES (JUNE 1975)

Table BI. Field data of Lake Powell water samples.

Water sample	Location on map	Date Collected	pH	Temperature (°C)	Secchi disk depth (m)
Dark Canyon	1	12 June	8.10	-	.09
Mille Crag Bend-Mile 175	2	"	-	-	.18
Hite Bridge-Mile 171	3	"	8.20	18.0	.18
Dirty Devil River	4	"	-	-	-
Dirty Devil-Bay	5	"	-	-	-
Dirty Devil-Mile 170	6	"	8.50	-	-
North Wash River	7	13 June	-	-	-
North Wash-Middle	8	"	-	-	-
Mile 168	9	12 June	8.50	18.0	.30
Mile 168 (clearer water)	10	"	-	-	.50
Mile 165	11	"	8.58	23.0	.50
Mile 160	12	"	8.40	21.0	-
Mile 155	13	"	8.40	19.6	.50
Castle Butte	14	11 June	8.55	21.5	.75
Mile 150	15	"	8.60	20.0	.75
Good Hope	16	"	8.68	21.0	-
Good Hope-Mile 145	17	"	8.82	21.2	1.0
Mile 140	18	"	8.50	18.0	1.0
Mile 136-Tapestry Wall	19	"	8.50	18.5	0.9
Tapestry Wall-surface	20	14 June	8.50	25.0	1.5
" " 31 m	20	"	8.05	15.0	-
" " 37 m	20	"	8.20	13.0	-
" " 46 m	20	"	8.15	10.5	-
" " 76 m	20	"	7.95	8.8	-
" " 86 m	20	"	7.90	9.8	-
Hansen Creek-Mile 130	21	11 June	8.45	17.7	1.0
Moki Canyon-Mile 125	22	15 June	-	-	2.5
Bullfrog Creek-Mile 122	23	10 June	-	-	-
" "	23	"	-	20.0	-
Bullfrog Bay	24	9 June	8.62	20.0	-
Beehive Rock-surface	25	16 June	8.62	22.5	3.75
" " 3 m	25	"	8.62	22.0	-
" " 15 m	25	"	8.25	17.5	-
Instrument Raft-surface	26	10 June	-	-	4.0
" " "	26	16 June	8.62	23.0	4.5
" " 3 m	26	"	8.62	21.5	-
" " 15 m	26	"	8.25	18.0	-
Bullfrog Buoy	27	"	-	23.5	3.5
Hall's Crossing	28	15 June	8.60	23.5	2.8
Mile 110	29	"	-	-	4.5
Rincon-Mile 101	30	"	8.55	26.0	4.0

Table BII. Field determinations of percentage of light transmittance.

Water sample	Light transmittance (%)													
	.400μ	.425μ	.450μ	.475μ	.500μ	.525μ	.550μ	.575μ	.600μ	.625μ	.650μ	.675μ	.700μ	Average
Dark Canyon	10	11	13	12	12	12	14	15	16	15	15	15	15	13.5
Mille Crag Bend-Mile 175	12	14	16	17	16	13	21	24	25	27	30	34	35	21.8
Hite Bridge-Mile 171	18	21	22	25	24	29	31	33	40	42	42	44	45	32.0
Dirty Devil River	0	0	0	0	0	0	0	0	0	0	0	0	0	0
Dirty Devil-Bay	80	84	88	89	93	93	95	93	93	93	96	97	97	91.6
Dirty Devil-Mile 170	72	74	78	79	82	75	82	78	88	85	95	95	95	82.9
North Wash River	-	-	-	-	-	-	-	-	-	-	-	-	-	-
North Wash-Middle	82	82	88	84	86	84	86	90	88	88	92	93	94	87.5
Mile 168	44	49	52	52	56	61	61	63	68	66	70	77	77	61.2
Mile 168 (clearer water)	80	83	88	88	86	91	95	94	88	93	93	97	99	90.4
Mile 165	66	71	73	74	73	73	80	84	83	86	85	86	92	74.7
Mile 160	63	56	73	74	69	75	76	76	83	83	80	82	83	74.8
Mile 155	74	68	73	71	80	82	78	83	80	83	84	80	84	78.5
Castle Butte	85	84	84	82	89	86	90	89	90	94	93	94	93	88.7
Mile 150	79	84	87	87	93	93	90	97	97	96	97	97	98	91.9
Good Hope	86	92	96	96	90	92	96	88	90	95	99	99	100	93.8
Good Hope-Mile 145	85	86	87	88	89	90	92	92	94	94	94	94	94	90.7
Mile 140	81	86	87	90	91	92	93	94	94	94	94	94	98	91.4
Mile 136-Tapestry Wall	-	-	-	-	-	-	-	-	-	-	-	-	-	-
Tapestry Wall-surface	80	88	90	87	90	90	92	93	94	95	94	95	96	91.1
" " 31 m	-	-	-	-	-	-	-	-	-	-	-	-	-	-
" " 37 m	-	-	-	-	-	-	-	-	-	-	-	-	-	-
" " 46 m	-	-	-	-	-	-	-	-	-	-	-	-	-	-
" " 76 m	-	-	-	-	-	-	-	-	-	-	-	-	-	-
" " 86 m	4	5	7	8	10	9	11	15	17	18	19	23	27	13.3
Hansen Creek-Mile 130	78	83	92	88	90	87	93	91	96	99	98	99	98	91.7
Moki Canyon-Mile 125	-	-	-	-	-	-	-	-	-	-	-	-	-	-
Bullfrog Creek	89	90	92	92	92	94	94	94	94	96	96	98	98	93.8
" "	-	-	-	-	-	-	-	-	-	-	-	-	-	-
Bullfrog Bay - Mile 122	92	92	93	96	98	99	100	100	100	100	100	100	100	97.7
Beehive Rock-surface	92	96	98	98	94	95	99	97	99	94	96	100	100	96.8
" " 3 m	94	97	100	96	100	97	-	-	-	-	-	-	-	97.3
" " 15 m	92	99	98	100	96	95	-	-	-	-	-	-	-	96.7
Instrument Raft-surface	95	95	94	96	96	96	100	100	100	100	100	100	100	97.8
" " "	90	89	89	95	94	95	96	97	98	98	98	98	98	95.0
" " 3 m	92	92	97	97	96	100	100	100	98	98	100	98	100	97.5
" " 15 m	90	94	99	99	99	99	100	99	100	100	100	100	100	98.4
Bullfrog Buoy	94	100	100	100	96	100	-	-	-	-	-	-	-	98.3
Hall's Crossing	-	-	-	-	-	-	-	-	-	-	-	-	-	-
Mile 110	-	-	-	-	-	-	-	-	-	-	-	-	-	-
Pinyon-Mile 101	-	-	-	-	-	-	-	-	-	-	-	-	-	-

Table BIII. Laboratory determinations of percentage of light transmittance.

Water sample	Light transmittance (%)																		
	.400μ	.425μ	.450μ	.475μ	.500μ	.525μ	.550μ	.575μ	.600μ	.625μ	.650μ	.675μ	.700μ	.725μ	.750μ	.775μ	.800μ	.825μ	Average
Dark Canyon	19.5	20.9	22.3	23.9	25.2	26.5	28.0	29.2	30.5	31.5	32.5	33.5	35.9	38.2	39.5	40.5	41.1	41.5	31.1
Mille Crag Bend-Mile 175	31.2	33.2	35.1	37.0	38.8	40.4	42.0	43.9	45.1	46.3	47.5	48.8	51.0	53.2	54.5	55.7	56.5	56.8	45.4
Hite Bridge-Mile 171	39.2	41.2	43.1	45.2	47.1	48.8	50.1	51.9	53.0	54.4	55.6	56.6	58.7	60.3	61.5	62.5	63.3	63.4	53.1
Dirty Devil River	0.4	0.4	0.4	0.4	0.4	0.5	0.5	0.5	0.7	0.8	0.9	1.0	1.3	1.8	2.0	2.2	2.4	2.7	1.1
Dirty Devil-Bay	91.9	92.9	93.8	94.7	95.1	95.7	96.0	96.2	96.7	96.8	97.0	97.2	97.7	97.5	97.9	98.1	98.2	98.7	96.2
Dirty Devil-Mile 170	85.1	86.8	87.8	89.2	90.0	90.9	91.0	91.9	92.2	93.0	93.0	93.9	94.2	94.8	95.1	95.1	95.9	96.0	92.6
North Wash River	98.1	-	-	-	99.5	-	-	-	99.8	-	-	-	99.5	-	-	-	98.5	-	99.0
North Wash-Middle Mile 168	90.9	92.1	93.2	94.1	94.9	95.3	95.6	95.9	96.0	96.2	96.7	96.9	97.0	97.1	97.2	97.3	97.3	97.1	95.6
Mile 168 (clearer water)	64.1	66.1	67.9	69.7	71.2	72.2	73.5	74.9	75.8	76.6	77.2	78.2	79.5	80.5	81.5	82.0	82.1	82.1	75.3
Mile 165	94.3	95.2	96.4	97.2	97.7	98.0	98.2	98.2	98.3	98.5	98.7	98.9	98.9	98.9	98.9	99.0	99.0	99.0	98.0
Mile 160	82.8	84.0	85.3	86.3	87.1	88.0	88.9	89.2	90.0	90.3	90.8	91.5	92.0	92.8	92.8	93.2	93.2	93.7	89.6
Mile 155	80.9	82.4	84.0	85.1	86.1	87.0	87.8	88.2	89.0	89.8	90.0	90.5	90.1	91.8	92.1	92.5	92.8	93.1	58.5
Castle Butte	87.2	87.7	88.8	89.9	90.7	91.0	91.8	92.2	92.7	92.9	93.2	94.0	94.3	94.9	95.2	95.5	95.9	96.2	92.4
Mile 150	90.6	92.0	93.0	93.9	94.8	95.0	95.2	95.9	96.0	96.2	96.4	96.8	97.0	97.1	97.2	97.8	98.0	98.0	95.6
Good Hope	89.7	90.8	92.1	93.0	93.8	94.3	94.9	95.1	95.8	96.0	96.2	97.8	98.1	98.1	98.3	97.8	97.9	98.1	95.4
Good Hope-Mile 145	95.5	-	-	-	97.8	-	-	-	98.0	-	-	-	98.2	-	-	-	98.1	-	97.5
Mile 140	94.2	95.2	96.3	96.9	97.7	98.0	98.0	98.2	98.4	98.5	98.6	99.2	99.1	99.1	99.0	99.5	99.8	100.0	98.1
Mile 136-Tapestry Wall	92.2	93.5	94.7	95.2	95.0	96.2	96.8	97.0	97.2	97.2	97.6	98.0	98.5	98.5	98.6	99.0	99.1	99.5	96.9
Tapestry Wall-surface	95.5	-	-	-	98.9	-	-	-	99.0	-	-	-	98.8	-	-	-	99.1	-	98.3
" " 31 m	93.1	94.2	95.4	96.0	96.3	96.6	97.3	98.0	97.9	98.1	98.4	98.9	98.9	99.0	99.0	99.1	99.2	99.7	97.5
" " 37 m	93.8	95.0	95.7	96.2	96.8	96.8	97.3	97.7	98.1	98.2	98.1	98.5	98.9	98.9	99.1	99.1	99.5	99.5	97.6
" " 46 m	97.1	97.8	97.8	98.5	98.7	98.8	99.0	98.9	99.4	99.2	99.4	99.9	100.0	100.0	100.0	100.0	100.0	100.0	99.1
" " 76 m	97.5	97.6	97.8	93.2	98.2	98.0	98.9	99.5	99.4	99.5	99.7	100.0	100.0	100.0	100.0	100.0	100.0	100.0	99.1
" " 86 m	97.1	97.8	98.5	98.8	99.0	98.9	99.1	99.3	99.2	99.5	99.6	99.8	100.0	100.0	100.0	100.0	100.0	100.0	99.3
Hansen Creek-Mile 130	9.2	10.1	11.0	12.2	13.3	14.5	15.9	17.0	18.1	19.2	20.2	21.5	23.7	26.0	27.3	28.3	29.5	30.0	19.3
Moki Canyon-Mile 125	94.0	95.3	96.2	97.1	97.8	98.1	98.3	98.5	98.5	98.9	99.0	99.2	99.4	99.5	99.5	99.7	100.0	100.0	98.3
Bullfrog Creek	88.1	-	-	-	92.9	-	-	-	94.9	-	-	-	96.1	-	-	-	97.6	-	93.9
" "	91.1	92.9	93.8	94.2	95.0	95.2	95.9	96.0	96.3	96.2	96.3	96.7	97.0	97.0	97.3	97.1	98.7	98.8	95.9
Bullfrog Bay-Mile 122	47.9	48.9	49.8	50.8	51.9	52.9	54.0	54.1	55.8	56.5	57.2	58.3	60.1	61.9	63.0	63.8	64.5	64.8	56.5
Beehive Rock-surface	97.3	97.7	98.2	98.5	99.0	99.1	99.5	99.5	99.0	99.1	99.1	99.2	100.0	100.0	100.0	100.0	100.0	100.0	99.2
" " 3 m	95.5	96.3	96.7	97.2	97.3	97.5	98.0	98.2	98.8	98.8	98.9	99.0	99.0	99.0	99.0	99.0	99.0	99.0	98.1
" " 15 m	96.2	97.1	97.7	98.1	98.4	98.4	98.8	99.0	99.2	99.2	99.2	99.2	99.3	99.5	99.5	99.5	99.5	99.5	98.7
Instrument Raft-surface	96.4	96.4	97.0	97.7	97.9	98.1	98.3	98.6	98.6	98.8	98.9	99.0	99.0	99.0	99.0	99.0	99.1	99.2	98.3
" " "	96.9	97.3	97.9	98.4	98.6	99.1	99.1	99.5	99.3	99.3	99.3	99.8	99.7	99.5	99.7	99.9	100.0	100.0	99.1
" " 3 m	95.4	96.0	96.7	97.2	97.6	97.8	98.1	98.5	98.9	98.9	98.6	98.8	99.0	98.9	99.0	99.0	99.2	99.5	98.2
" " 15 m	94.8	95.7	96.4	97.1	97.9	97.0	97.8	98.1	98.2	98.5	98.7	98.9	98.9	99.0	98.8	98.8	98.9	99.2	97.9
Bullfrog Buoy	94.0	95.1	96.1	96.8	97.4	97.8	98.2	98.2	98.5	98.5	98.9	99.0	99.0	99.0	99.0	99.0	99.0	99.0	97.9
Hall's Crossing	95.7	96.7	97.5	98.0	98.1	99.0	99.0	98.9	99.3	99.1	99.6	99.9	100.0	100.0	100.0	100.0	100.0	100.0	98.9
Mile 110	90.4	-	-	-	94.9	-	-	-	96.2	-	-	-	96.9	-	-	-	97.8	-	95.2
Rincon-Mile 101	92.8	-	-	-	96.1	-	-	-	97.0	-	-	-	97.5	-	-	-	97.6	-	96.2
	96.4	97.2	97.8	98.0	98.3	98.8	99.0	98.9	99.5	99.2	99.1	99.5	99.8	99.8	100.0	100.0	100.0	100.0	99.0